The Cryosphere Discuss., 8, 581–640, 2014
www.the-cryosphere-discuss.net/8/581/2014/
doi:10.5194/tcd-8-581-2014

The Cryosphere Discussions
Open Access

Projected changes of snow conditions and avalanche activity in a warming climate: a case study in the French Alps over the 2020–2050 and 2070–2100 periods

H. Castebrunet[1,2,3], N. Eckert[2], G. Giraud[3], Y. Durand[3], and S. Morin[3]

[1]INSA de Lyon, Laboratoire LGCIE, 20 Avenue des Arts, Bât. J.C.A. Coulomb, 69621 Villeurbanne, France
[2]UR ETGR, IRSTEA/Université de Grenoble Alpes, BP 76, 38402 Saint Martin d'Hères, France
[3]Météo-France – CNRS, CNRM-GAME UMR 3589, Centre d'Etudes de la Neige, 1441 rue de la Piscine, 38400 Saint Martin d'Hères, France

Received: 25 November 2013 – Accepted: 26 December 2013 – Published: 23 January 2014

Correspondence to: H. Castebrunet (helene.castebrunet@insa-lyon.fr)

Published by Copernicus Publications on behalf of the European Geosciences Union.

Abstract

Projecting changes in snow cover due to climate warming ~~is~~ is important for many societal issues, including adaptation of avalanche risk mitigation strategies. Efficient modeling of future snow cover requires high resolution to properly resolve the topography. Here, we detail results obtained through statistical downscaling techniques allowing simulations of future snowpack conditions for the mid- and late 21st century in the French Alps under three climate change scenarios. Refined statistical descriptions of snowpack characteristics are provided with regards to a 1960–1990 reference period, including latitudinal, altitudinal and seasonal gradients. These results are then used to feed a statistical model of avalanche activity–snow conditions–meteorological conditions relationships, so as to produce the first prognoses at annual/seasonal time scales of future natural avalanche activity eventually based on past observations. The resulting statistical indicators are fundamental for the mountain economy in terms of changes anticipation.

At all considered spatio-temporal scales, whereas precipitations are expected to remain quite stationary, temperature increase interacting with topography will control snow-related variables, for instance the rate of decrease of total and dry snow depths, and the successive increase/decrease of the wet snow pack. Overall, with regards to the reference period, changes are strong for the end of the 21st century, but already significant for the mid-century. Changes in winter are somewhat less important than in spring, but wet snow conditions will appear at high elevations earlier in the season. For a given altitude, the Southern French Alps will not be significantly more affected than the Northern French Alps, so that the snowpack characteristics will be preserved more lately in the southern massifs of higher mean altitude.

Regarding avalanche activity, a general –20–30 % decrease and interannual variability is forecasted, relatively strong compared to snow and meteorological parameters changes. This decrease is amplified in spring and at low altitude. In contrast, an increase of avalanche activity is expected in winter at high altitude because of earlier wet

snow avalanches triggers, at least as long as a minimal snow cover will be present. Comparison with the outputs of the deterministic avalanche hazard model MEPRA shows generally consistent results but suggests that, even if the frequency of winters with high avalanche activity will clearly decrease, the decreasing trend may be less strong and smooth than suggested by the changes in snowpack characteristics. This important point for risk assessment pleads for further work focusing on shorter time scales. Finally, small differences between different climate change scenarios show the robustness of the predicted avalanche activity changes.

1 Introduction

In temperate mountainous areas, snow is a major component of the water cycle. As an important element of the critical zone at the interface between atmosphere, geosphere, ecosystems and human societies, it has key impacts on geomorphological processes, biodiversity and tourism industry. As a consequence, since high altitude areas have been shown to be highly sensitive to climate change (Beniston, 2003), understanding the responses of the snowpack to the ongoing warming, related impacts and potential feedbacks (e.g. albedo change) is of major environmental (e.g Keller et al., 2005) and economic (e.g. Elsasser and Buerki, 2002; Gonseth, 2013) interests. This can be achieved by studying links between climate and snow cover for present conditions, which includes an assessment of changes already measurable using various observation series, and by quantifying changes to be expected in the (near) future using snow and climate simulations fed by climate change scenarios.

Recent climate change in mountainous areas is now fairly well documented, for instance in the European Alps (e.g. Beniston et al., 1997). Even if it has not been constant, with periods of slow temperature increase or even cooling, the warming since the end of the Little Ice Age ($\sim$ 1850) has been marked, and accelerated over the 1985–2000 period (e.g. Beniston, 2005a). Following studies at larger spatial scales (e.g. Brown, 2000; Mote, 2003; Hungtington et al., 2003; McCabe and Wolock, 2002),

several studies have documented consecutive decreases in snow precipitation phase, snow depths, snow cover durations or snow water equivalent in many countries of the Alpine space (e.g. Falarz, 2002, 2004; Laternser and Schneebeli, 2003; ONERC, 2008; Valt and Cianfarra, 2010). Increased variability has also been observed, especially for winter temperatures, inducing an increasing number of warm winter spells (Beniston, 2005b). Lastly, efforts have been made to quantify elevation-dependent effects on warming (Rangwala and Miller, 2012) and their complex interaction with the freezing level, leading to less marked trends in snow variables at high altitude (Moran-Tejeda et al., 2013). For the specific case of the French Alps, a rather complete picture of recent changes is available, including sub-regional, altitudinal and seasonal gradients thanks to systematic point measurement analysis (Dumas, 2012; Gaume et al., 2013) ~~and~~ snow and meteorological retrospective analyses and simulations (Durand et al., 2009a, b).

Concerning future snow evolution, first estimations have been obtained through simple extrapolations of current observed trends (e.g. Beniston et al., 2003) or sensitivity studies using snow models (Martin et al., 1994). More detailed future snow simulations using climate change scenarios as input have emerged recently (e.g. Lopez Moreno et al., 2009, 2011; Bavay et al., 2009), allowing better quantification of the changes to be expected. They highlight, in addition to intuitive consequences of warming such as wetting and a strong decrease of snow cover, other important effects such as an increase of heavy snowfall at high altitude or a much narrower snow melt discharge peak in spring. However, strong difficulties still remain, making prognoses regarding snow evolution still debated (Räisänen, 2008). Among these, the main obstacle in many impact studies is the difficulty of modeling climate at relevant spatial scales (Rousselot et al., 2012). Indeed, most of the 21st century projections rely on global climate models (GCMs) whose typical scale (150–300 km) is by far too large when working in mountain areas for which a much higher resolution is required to properly resolve the topography.

Among the geomorphic processes controlled by snow and meteorological variables, and, on longer time scales, by climate, natural avalanche activity strongly impacts

mountain communities through the related risk for humans and infrastructures. Hence, possible occurrence of catastrophic events (e.g. SLF Davos, 2000) under ongoing climate change requires accurate adaptation strategies (Richard et al., 2010). However, quantifying the impact of the recent changes in mountain climate on natural avalanche activity and its future evolution in terms of possible modifications of the frequency and intensity of both ordinary and extreme events remains a rather open questions (Keiler et al., 2010; IPCC, 2012).

Past evidences of significant changes in real avalanche data series have been provided very recently, notably in the French Alps (Eckert et al., 2010a, b, 2013), with clear links to snow and meteorological changes (Castebrunet et al., 2012) and their altitudinal control (Lavigne et al., 2012, 2013). Regarding future evolution for the 21st century, at our knowledge, the only existing results are those of Martin et al. (2001) and Lazar and Williams (2008). They both suggested an ongoing increase in the proportion of wet snow avalanches with regards to dry snow avalanches, and a shift in their timing, in good correlation with field observation of snow cover wetting at small scale and its link with wet snow release susceptibility (Mitterer et al., 2011), but without a clear quantification of the amplitude of change in total avalanche activity.

To evaluate the potential impact of global change on snow conditions in the French Alps for the forthcoming decades through numerical simulations at relevant spatial scales, Rousselot et al. (2012) have developed statistical adaptation techniques. Specifically, an analogue method has been applied to high resolution regional climate model predictors so as to provide complete, physically consistent time-series of meteorological variables needed for physically-based snowpack modeling.

~~Grounding on this work~~, the current study aims at producing a detailed statistical description of refined snowpack characteristics expected in the French Alps in mid and end-21st century, including latitudinal, altitudinal and seasonal gradients and under three greenhouse gas (GHG) emissions hypotheses. These results are also used to feed statistical models developed by Castebrunet et al. (2012) to link avalanche activity and the snow and meteorological data produced by the SAFRAN–Crocus–

MEPRA model chain (see below). Hence, future changes in avalanche activity at annual/seasonal time scales are compared to the 1960–1990 control period on the basis of natural, actually observed, avalanche activity and simple but robust statistical relations.

2 Data and methods

2.1 Past meteorological, snow and avalanche data at the massif scale

The primary data used in this study consists of daily observed and simulated past snow and meteorological data and avalanche counts over the French Alps, at the geographical scale of the 23 massifs of the French Alps used for avalanche forecasting in an operational context (Fig. 1). The surface area of each massif is about 500 km^2, and the key assumption regarding snow and meteorological numerical simulations is their spatial homogeneity.

Daily observed avalanche data come from the "Enquête Permanente sur les Avalanches" (EPA) which describes the avalanche events on approximately 3900 designated paths in the French Alps and Pyrenees since the beginning of the 20th century (Mougin, 1922). The most common use for EPA data is hazard (e.g. Ancey et al., 2004; Eckert et al., 2007a) and risk (e.g. Eckert et al., 2009) assessment at the path scale. However, the EPA is also well suited for large-scale studies on relations with snow and meteorological covariates (Jomelli et al., 2007), major avalanche cycles (Eckert et al., 2010c) and spatial variations in avalanche activity (Eckert et al., 2007b). For climate studies, the major advantages of the EPA are the long time span of the available data series in a context of a well-structured observation network, giving a relatively accurate view of the spatiotemporal fluctuations of natural avalanche activity in France over the last century. Various quantitative (run out elevations, deposit volumes, etc.) and qualitative (flow regime, snow quality, etc.) data (Jamard et al., 2002) are recorded. Sources of uncertainties and systematic errors in the estimation of certain variables

are numerous and detailed in previous studies (e.g. Eckert et al., 2010c; Castebrunet et al., 2012).

In this study, among all the available information, only avalanche counts, which is the most natural variable to describe the frequency of the phenomenon, are considered. In this case, the predominant source of error to be considered is missing events. Locally, the quality of the records depends to a large extent on careful data recording by local observers (mostly forestry rangers). However, once the avalanche counts are aggregated at the massif scale, these local heterogeneities are smoothed, making the automatic detection of abnormally low records very difficult. For instance, of all the local series, no error-free modeled series is available so that homogenization methods (e.g. Caussinus and Mestre, 2004) are difficult to implement and were not used in this study. This must be kept in mind when interpreting results. It is generally admitted that the EPA chronicle underestimates avalanche activity at high elevations because human observations concern mainly paths selected to be visible from valley floors. This is another potential source of bias.

Daily snow and meteorological conditions consist of outputs from retrospective snow and meteorological analyses with the SAFRAN–Crocus–MEPRA (SCM: Durand et al., 1999, 2009a, b) model chain. The meteorological analysis is performed at the scale of the massifs shown in Fig. 1 for which meteorological conditions are assumed to be homogeneous but may vary with altitude. Durand et al. (2009a, b) performed a complete reanalysis of meteorological and snow conditions with SCM using 44 yr of analyzed atmospheric model data from the 40 yr European Centre for Medium-Range Weather Forecast (ECMWF) reanalysis (ERA-40) project (Uppala et al., 2004) completed by observation datasets extracted from the operational databases of Météo-France. This reanalysis, complemented for years beyond the end date of the ERA-40 dataset using large-scale meteorological fields from Météo-France operational numerical weather prediction models, covers the period from 1958 to 2009 and is referred to as the *SCM-ERA40* model run. For the present study, the following variables were used, similar to those described by Castebrunet et al. (2012). They concern the 23 alpine massifs

(Fig. 1), for three elevations: 1800, 2400, and 3000 m a.s.l., leading to 57 variables in total:

- Daily cumulated precipitation (rain and snow), temperature (daily minimum, maximum, and mean), maximum daily wind speed, and the associated direction (SAFRAN outputs).
- For the four main aspects (northern, eastern, southern, and western) and a 40° slope, the total snow depth, the thickness of surface wet snow and the thickness of surface recent dry snow. These variables are derived from outputs of the detailed snowpack model Crocus fed by SAFRAN meteorological conditions (Brun et al., 1992). The thickness of surface wet snow is taken as the sum of the thickness of the contiguous wet snow layers characterized by a liquid water content greater than 0.01 % from the surface. The thickness of the surface recent dry snow is the depth of the deepest snow layer characterized by a dendricity greater than 0.25.
- Natural snowpack instability through the MEPRA index which gives information of the avalanche hazard without being certain that a triggering actually occurred (Giraud, 1993; Durand et al., 1999). MEPRA is a diagnostic tools assessing snowpack stability based on Crocus simulated snow stratigraphy. MEPRA outputs, which are computed within each massifs for each slope, altitude and aspect classes, are aggregated at the massif scale thereby providing a single scalar value for a given date. The MEPRA index, called hereafter MI, varies between 0 and 8, and is somewhat dependent on massif characteristics. For example, the highest values are obtained in the highest massifs, where snowfalls are the most intense, leading to higher instability. The MI can be viewed as a synthetic combination of SAFRAN/Crocus snow and meteorological data relevant to estimating avalanche susceptibility rather than a true measure of avalanche activity. It is important to keep in mind that the MI is used in an operational context to help forecasting of potential snowpack instability and so has to be sensible to snow and weather conditions when avalanche hazard is important. On the other hand, this index is less

sensitive to weak instability or sporadic events at the massif scale, as discussed in Castebrunet et al. (2012).

2.2 Relating avalanche activity to snow and meteorological covariates through regression models at large spatio-temporal scales

Castebrunet et al. (2012) proposed a time-implicit approach for the detection of abnormal years and low-frequency trends in various indicators of natural avalanche occurrence: EPA counts, MEPRA index and a composite index, see below. The best explanatory snow and meteorological covariates were picked up with a stepwise regression (e.g. Saporta, 2006), i.e. a variable selection procedure for linear models in which the set of predictive variables is retained by an automatic sequence of Fisher F tests. The regression model obtained relates the series y_t of avalanche activity indicators to P selected standardized explanatory variables X_{jt}^{norm} such as:

$$y_t = \sum_{j=1}^{p} X_{jt}^{\mathrm{norm}} \beta_j + \varepsilon_t, \tag{1}$$

with β_j the weighting coefficient representing the contribution of each predictive variable retained to the fluctuations of avalanche activity, and ε_t the residual activity not predicted by the model. The values of ε_t are modeled as independent and identically distributed realizations of a centered Gaussian random number with standard deviation σ. The function $\sum_{j=1}^{p} X_{jt}^{\mathrm{norm}} \beta_j$ seen as a time series shows temporal fluctuations that are clearly related to the temporal fluctuations of the covariates, hence providing a better understanding of the response of avalanche activity to changes in its most important drivers than a direct time series analysis of the y_t series.

Rather than focusing on daily counts at the massif scale, Castebrunet et al. (2012) considered larger spatio-temporal scales. Annual (15 December to 15 June) and seasonal (winter and spring) series of anomalies were built for the whole French Alps (all 23

French massifs), the Northern French Alps, and the Southern French Alps (Fig. 1). Winter and spring sub-seasons are defined as the 15 December to 14 March and 15 March to 15 June sub-periods, respectively. At these scales, regression models were derived from *SCM-ERA40* outputs over the period 1958–2009. Analysis and validation showed that they were able to represent both high and low peaks and low-frequency trends, indicating a clear statistical relation between the fluctuations of avalanche activity and those of the selected covariates, a somewhat surprising result given that the avalanche release process is a strongly discontinuous response to meteorological patterns and changes in snowpack characteristics. Hence, it looks like averaging over large areas and relatively long periods smoothes this process, switching from meteorological and snow control to climatic control, and making it possible to capture the predominant factors for the long-term interannual evolution with simple statistical regression models. The same study showed also that good correlations exist between EPA avalanche counts and the MEPRA index (MI) during cold and dry winter periods, taking into account the fact that avalanche counts are then often underestimated. In contrast, it was found that the MI often fails to capture avalanche activity due to wet snow conditions during spring or temporally or spatially more sporadic avalanche events. As regression models used annual or seasonal anomalies, some of these biases could be significant. To limit them, a composite index referred to as CI was proposed to combine EPA and MI avalanche activity indicators and better represent the overall natural activity. It is computed using the annual anomalies of the instability index $\mathrm{MEPRA}_t^{\mathrm{norm}}$ and avalanche counts $\mathrm{EPA}_t^{\mathrm{norm}}$, and the correlation coefficient ρ_t between their daily values during the year/season:

$$\mathrm{CI}_t = \frac{1}{3}(0.5\mathrm{EPA}_t^{\mathrm{norm}} + 0.5\mathrm{MEPRA}_t^{\mathrm{norm}} + \rho_t). \tag{2}$$

It gives similar weight to EPA counts and the MI, and favors/disadvantages years or seasons where they are coherent/incoherent, respectively. Standardization is used to spread the values over a $[-2,2]$ range similar to the one corresponding to the explanatory variables. Finally, while the CI is primarily computed at the massif scale, obtaining

spatially averaged time series is straightforward, assuming similar weights for all massifs.

Grounding on this work, we assume in this study that the CI is the best indicator of natural avalanche activity and we base the assessment of future changes in avalanche activity on it for the same nine spatio-temporal scales (3 regions/3 periods, see Sect. 3). We will however check and discuss the consistency of the patterns we highlight with the annual/seasonal changes using the MI which can be easily computed for the future period from the simulations of future snow characteristics, in contrast to EPA data which by nature are only available for past years. In addition to the work already reported by Castebrunet et al. (2012), we developed new regression models with the same stepwise selection methodology, but considering the period 1961–1990 only (instead of 1958–2009) of the simulation SCM-ERA40. This was found necessary for (i) respecting the control period used for the climate projections (see Sect. 2.3), and (ii) enlarge the temporal gap between the reference 1961–1990 and the 2020–2050 periods.

The obtained nine new CI regression models are summarized in Tables 1–3. All determination coefficients are very good (higher than 0.7), which illustrates the relevance of explaining avalanche activity with a few (from one to nine) snow and meteorological covariates. At a very global scale (entire French Alps and whole avalanche year, Table 1), the CI model (determination coefficient $R^2 = 0.91$) includes 4 snow variables, all of which related to Northern slopes. Only snow depth at 2400 m has a negative contribution to the avalanche activity indicator CI. More variables are required to explain the CI for the Northern French Alps (9, vs. 4 for the Southern French Alps). They concern different slope orientations (north, east, west) and maximal daily temperatures at mid and high elevations in addition to snowpack characteristics. For the Southern French Alps, the CI model includes snow precipitation at 3000 m and snowpack variables for north and west slopes.

Regarding the winter period, CI models for the three regions are characterized by a limited number of covariates related to thickness of snow (1 to 3), and by the predominant contribution of the thickness of surface recent dry snow at 3000 m for east-

ern slopes (marginal correlation with the composite index $\rho_j > 0.8$). This highlights that this season is dominated by fresh dry snow avalanches. While for the Northern French Alps the statistical model only includes the thickness of surface recent dry snow, the thickness of wet snow for Northern slopes also contributes to the statistical models at the scales of both the entire French Alps and Southern French Alps.

For the spring period, more variables are required to adequately explain the annual fluctuations of the CI (2 to 5). They concern snowpack characteristics, mainly at mid and high elevations. For instance, two among four variables are thicknesses of wet snow for the Northern French Alps, which is logical as spring avalanches are mainly wet snow avalanches. Notably, this is not the case for the Southern French Alps, but the total snow depth for a south facing slope which is included in the model may play a similar role.

The efficiency and robustness of the 9 regression models have been evaluated and checked on the 30 yr calibration sample using a leave-one-out validation scheme. In the latter, each "data" (year) is successively removed from the calibration sample, the model is fitted without it, and it is then predicted with the fitted model. Figure 2 shows the predictive performance of three statistical models corresponding to the different regions/time periods studied. Nearly all predicted values fall in the 95 % confidence intervals around the data (the traditional ± two standard deviations in a linear regression), and predictions obtained during the validation procedure are very close to the ones obtained when the whole data set is used for calibration.

Table 4 quantifies and generalizes these statements, showing that, for all the models, nearly "perfect" success rates are obtained in calibration, i.e. around 95 % of the predictions falling in the 95 % confidence intervals around the data. In the leave-one-out cross validation procedure, success rates are unsurprisingly a bit lower, but remain as high as ∼ 90 %, showing that in each region/period, the model is correctly able to predict nearly all observations without the data corresponding to each observation. These results can be considered very satisfactory with regards to the relative roughness of the statistical modeling approach employed. They give confidence in the fitted relationships between

avalanche activity and meteorological and snow conditions, and their ability, despite their arguable oversimplification, to roughly reproduce different avalanche triggering contexts, at least for the climate of the reference period (see Sect. 4 for discussion about their validity under future climate).

2.3 Modelling climate, snowpack characteristics and avalanche activity in the future

In order to carry out projections of the impact of climate change on snow conditions and avalanche activity in the French Alps, the model chain SAFRAN–Crocus–MEPRA (SCM) was run using as input dynamically downscaled variables from the regional climate model (RCM) ALADIN-climate-V4 (Rousselot et al., 2012) for a limited area at 12 km resolution. This was made to specifically study mountain climate and its impacts on the evolution of snow cover in France.

Three running periods have been considered: the reference period (1961–1990) and two future periods, mid- and late 21st century (2021–2050 and 2071–2100) according to three 4th IPCC (IPCC, 2007) emission scenarios (IPCC Special Report on Emissions Scenarios SRES B1, A1B and A2):

- the A1B scenario describes a future world with rapid, globalized economic growth, the development of new, more efficient technologies, and a global population increase until mid-century with decline thereafter;
- the A2 scenario assumes regionally heterogeneous economic and technological development throughout the world and a continuously increasing population. This is one of the most greenhouse gases (GHG) emissive IPCC scenarios;
- the B1 scenario assumes similar evolution of the global population to that in A1B, but with an economy dominated by services and information activities and the use of clean technologies. This scenario is the least emissive one, with GHG emissions that are stabilized before the end of the century.

Since A1B scenario is the closest to the 2050 forecasts of the International Energy Agency, we mainly focus on this scenario in this work, but the three of them were tested and the results are briefly reported in Sect. 3.

The ALADIN RCM boundary conditions were provided by the global ARPEGE-climate-V4 GCM (Deque and Somot, 2007) running with a variable horizontal resolution of about 50 km over Europe. The sea surface temperature used for coupling ALADIN to ARPEGE originates from previous coarser resolution runs of ARPEGE. The reference period (called EM6) is a continuous ALADIN simulation between 1961 and 1990, whereas both future climatic periods 2021–2050 (called EM7) and 2071–2100 (called EM9) are simulations consisting of 30 "one-year-runs" (independent year which can exist under considered climatic period).

The SCM two steps downscaling procedure, based on these ALADIN fields, is largely described and discussed in Rousselot et al. (2012). It is composed of a nearest-neighbor research of similar meteorological situations (analogue day) and a two-levels statistical correction procedure in order to correct both the initial bias of the EM6 run and to insert the climate change signal. Firstly, for each simulation and each ALADIN grid point, meteorological daily outputs are compared with daily data from ECMWF ERA-40 reanalyzes (Uppala et al., 2004) and a date with analogue weather conditions is identified through an appropriate distance. The series of analogues dates is then used to extract corresponding meteorological data from the SCM-ERA40 meteorological reanalysis (Durand et al., 2009a) that we call $\mathrm{EM}x^{\mathrm{CS}}_{\mathrm{DATE}}$ with $x = 6$, 7 or 9 and CS the SRES scenario, namely A1B, A2 or B1.

Secondly, the meteorological variables are statistically corrected and adapted to the different elevations, aspects and slopes of the Alpine massifs with a percentile-percentiles approach (as explained in Deque, 2007) which uses the 99 percentiles of the SAFRAN meteorological variables (temperature, relative humidity, precipitation, cloudiness, wind) issued from the previous $\mathrm{EM}x^{\mathrm{CS}}_{\mathrm{DATE}}$ and SCM-ERA40 time series for each season. For consistency, the SCM-ERA40 data series used were limited to the 1960–1990 period. These percentiles (at rank α) are noted $q_\alpha(\mathrm{EM}x^{\mathrm{SC}}_{\mathrm{DATE}})$ and

$q_\alpha(\mathrm{SCM}^{\mathrm{ERA40}})$, respectively, and are used to produce ranked differences, at the same α percentile value, between the different RCM projections and the statistics of meteorological variables in the SCM-ERA40 record. The implicit assumption of this CENT method is that all the differences are evaluated at the same probability value (through the common α percentile) but are without impact on the temporal properties of the series due to the smoothed and ranked feature of the correction. For example if a field is less persistent than another one, their corrected values will keep this property.

The differences between RCM outputs and SCM-ERA40 reanalysis can be split in two components:

- the initial model bias, i.e. the difference between the percentiles of the control period simulation $\mathrm{EM6}_{\mathrm{DATE}}$ and the SCM-ERA40 simulation $\mathrm{SCM}^{\mathrm{ERA40}}$which is due to the fact that the ALADIN model in its EM6 run does not match the *SCM-ERA40* density function:

$$\delta_{\mathrm{model}} = |q_\alpha(\mathrm{EM6}_{\mathrm{DATE}}) - q_\alpha(\mathrm{SCM}^{\mathrm{ERA40}})|; \quad (3)$$

- the bias linked to simulated climate change signal, i.e. the difference between the percentiles of the future period simulation and the SCM-ERA40 simulation $\mathrm{SCM}^{\mathrm{ERA40}}$:

$$\delta_{\mathrm{CC}} = |q_\alpha(\mathrm{EM7,9}^{\mathrm{SC}}_{\mathrm{DATE}}) - q_\alpha(\mathrm{SCM}^{\mathrm{ERA40}})|. \quad (4)$$

Both corrections are applied on SAFRAN meteorological variables extracted for the relevant dates from simulation *SCM-ERA40*, leading to meteorological fields called $\mathrm{EM}x^{\mathrm{CS}}_{\mathrm{CENT}}$ as:

$$\mathrm{EM7,9}^{\mathrm{CS}}_{\mathrm{CENT}} = \mathrm{SCM}^{\mathrm{ERA40}} + \delta_{\mathrm{CC}} - \delta_{\mathrm{model}}. \quad (5)$$

In other words, the technique employed consists in adding to the climatologic field (*SCM-ERA40*) a correction representative of the difference between the ALADIN behavior between the present and the changed climatic conditions. This correction takes

into account the potential deficiencies of the $\mathrm{EM6}_{\mathrm{DATE}}$ run when compared to the *SCM-ERA40* climatology and we postulate that these modelling errors are the same in the climate changed runs $\mathrm{EM7,9}^{\mathrm{CS}}_{\mathrm{DATE}}$. This convenient assumption has been widely used in previous studies and is discussed for instance in Wilby et al. (1998) and Deque (2007). Anyhow, in the present work, we note that the magnitude of the δ_{model} correction is small for several variables (Rousselot et al., 2012).

Then, the meteorological fields $\mathrm{EM7}^{\mathrm{CS}}_{\mathrm{CENT}}$ and $\mathrm{EM9}^{\mathrm{CS}}_{\mathrm{CENT}}$ were used as inputs to drive the detailed snowpack model Crocus outputs and, subsequently, the MEPRA index, for the two considered "30 yr" future periods and under the three different SRES scenarios considered. Simulated SAFRAN and Crocus data from the daily series at the massif scale were used to derive anomaly series at the 9 larger spatio-temporal scales corresponding to those studied for the reference period. Obtained future samples of annual/seasonal means of the MEPRA index at the annual time scale are close to the ones briefly presented in Giraud et al. (2013), but evaluated with the additional CENT correction.

Finally, the nine CI regression models obtained over the reference period were fed with these projected snow and meteorological data (after suitable standardization), using appropriate weighting coefficients (Tables 1–3), leading to projected values of the avalanche activity index CI for the two future periods of annual and seasonal avalanche activity indexes for the nine regions/seasons considered. For example, Fig. 3 presents the distribution of annual and seasonal values of the CI regression model during the reference period and the two time periods considered in the future, at the entire French Alps scale. For the reference period, simulated values are shown as well as a reasonable smoothed approximation of their density function from a semi-parametric interpolation of the pseudo observations with a Gaussian kernel smoother. For the future period, for clarity, only the smoothed density functions are displayed.

2.4 Quantitative assessment of changes

Quantitative assessment of changes between the reference (1961–90) and the two considered future periods (2020–2050 and 2070–2100) was made for a selection of snow and meteorological variables at different elevations and expositions, for the Composite Index CI and for the MEPRA index MI (Tables 5–7).

More precisely, we computed normalized differences in means $\mathrm{Diff}^{\mathrm{means}}$ (differences between interannual means – respectively mean(Xt) and mean(Yt) where Xt and Yt are the two considered annual (or seasonal) samples) divided by a surrogate of the variability range as:

$$\mathrm{Diff}^{\mathrm{means}} = \frac{\mathrm{mean}(Yt) - \mathrm{mean}(Xt)}{\max(Xt) - \min(Xt)}, \quad (6)$$

and variance ratios as:

$$\mathrm{Diff}^{\mathrm{var}} = \frac{\mathrm{var}(Yt)}{\mathrm{var}(Xt)}. \quad (7)$$

Because of the computational burden, only 30 yr of past and future variables Xt and Yt from CENT simulations are available. This implies that significance of changes had to be tested thoroughly, as follows:

- the significance of differences between future and reference samples, using the Kolmogorov–Smirnov test;
- the significance of the difference in mean and variance using Fisher and Student tests.

According to the statistical theory, we applied Fisher and Student tests only for Xt samples for which the normality tested using the Shapiro Wilks test was not rejected at the 0.05 significance level. Due to the facts that we have only samples of 30 values and

that we are considering annual/seasonal means, the normality assumption was indeed acceptable most of the time, even for asymmetric variables such as snow depths which are generally not Gaussian. Similarly, according to its theoretical setting, the Student test for means was applied only when the assumption of non-significant differences in variances between the two considered Xt and Yt samples could not be rejected. Since variances between considered samples were often significantly different, this test could be applied less frequently. We also assessed probabilities for future years/seasons to exceed the mean and high percentiles of the distribution on the reference period. The exceedence probabilities were computed from the normal fit on the Xt samples when possible (i.e. when the Gaussian assumption could not be rejected), and from the Kernel smoothing approximation of the empirical cumulative distribution function (cdf) introduced previously otherwise. Finally, we also tested the difference between the multivariate distributions of annual/seasonal variables corresponding to each of the CI model (that is, for each of the 9 regression models, the joint distribution of the variables $X_{\mathrm{jt}}^{\mathrm{norm}}$, $j = [1, P]$ number of covariates) using the Cramer test (Table 8).

3 Results

3.1 Meteorological and snowpack conditions in the future

Meteorological and snow conditions in the future at the massif and annual scales are presented and discussed in details by Rousselot et al. (2012). Here, we complement the analysis by assessing changes between reference and future periods in terms of probabilities of exceeding percentiles of the distribution on the reference period in the future and by normalized differences and ratios for the 9 spatio-temporal scales we consider. We also expand the approach to snowpack variables more directly relevant for avalanche activity that were not considered in the previous study (e.g. snow conditions on slopes, and dry recent/wet surface snow thickness). Figures 4–8 illustrate regional north/south differences regarding to the whole French Alps while Table 5

shows detailed results for the entire French Alps only, but displaying results for the three considered time scales, highlighting seasonal variations. In what follows we focus on projections concerning the A1B scenario (IPCC, 2007) only.

In Table 5, it is important to note that differences in probabilities of exceeding percentiles can be insignificant if underlying distributions are not different (null hypothesis not rejected by the Kolmogorov–Smirnov test). Hence, significant differences are shown in bold. For the whole year, it is generally the case for all variables except for the total precipitations and for the thickness of wet snow at 3000 m for a south facing slope, for the latter only between reference and 2020–2050 periods. Similarly, normalized differences in interannual means and variance ratios are often high and far from one, respectively, but testing the significance of these changes could not always be done, depending on the Shapiro–Wilks and Fisher Test results. Significant differences are shown in bold whereas values whose significance could not be tested are shown in grey.

3.1.1 Temperatures

As expected, between the reference period and the mid-21st century, temperatures were found to increase significantly. This increase continues towards the end-21st century (2070–2100). The increase is very homogeneous over the Alps, concerns daily, minimal and maximal values as well as low and high elevations (Fig. 4). For example, at the annual scale and for the entire French Alps, standardized anomalies indicate a ∼ +60/75 % mean increase at the mid-21st century with regards to the reference period. Hence, the mean over the reference period is already exceeded almost surely for all the years simulated under this changed climate. Even more impressively, the 75 % percentile of the reference sample is exceeded for nearly all the years simulated for the end-21st century with a ∼ +115/155 % mean increase in standardized anomaly with regards to the reference period. On the other hand, increase during winter sub-season is expected to be a bit less important than during spring sub-season, e.g., for the entire French Alps, +40–55 % vs. +65–90 % mean increase towards the end-21st century in

winter/spring, respectively (Table 5). For all periods/seasons, variance ratios are within the 0.8–1.2 range, indicating moderate and often insignificant changes not higher than 20 % in interannual variability, even between the reference period and the end-21st century (Table 5).

3.1.2 Total and snow precipitation

Climate change has little effect on total precipitation at any considered spatio-temporal scales with changes almost always insignificant in distribution/mean/interannual variability with regards to the reference period, even towards the end-21st century (Fig. 5 and Table 5). It can only be noted that differences in mean standardized anomalies are always negative, with maximal amplitude of around −15 % for the Southern French Alps towards the end-21st century. In contrast, the phase of the precipitation is strongly impacted by warming, leading to rather strong decreases in snow precipitations. This is especially true at low elevations, during spring with regards to the winter period (Table 5), and, at a lower extent, for the Southern French Alps with regards to the Northern ones (Fig. 5). The reason is that, for a given altitude, the solar radiation is stronger in spring and/or for south region. Expectedly, the decrease goes on with warming from the mid to the end-21st century. Noteworthy, the reduction in mean is also accompanied by a rather strong decrease in interannual variability, because annual snowfall much higher than the interannual mean become more and more seldom. For example, for the entire French Alps at annual scale, at 1800 m, the decrease in mean standardized anomaly is around −30 and −50 % towards the mid and end-21st century, respectively, with a variance ratio between the end-21st century and the reference period of only 0.4. These changes lead to the fact that, for the end-21st century one expects no longer any year with total snowfall as high as the mean over the reference period (Table 5). Note, however, that changes are much smaller at high altitudes, because temperature increase is then not sufficient to significantly impact the precipitation phase (Fig. 5 and Table 5).

3.1.3 Total snow depth

Concerning snowpack characteristics, following snow precipitation changes, total snow depths in future strongly decrease in terms of distribution, interannual mean and interannual variability (Fig. 6). Expected changes are stronger between the reference period and the mid-21st century than between mid and end-21st century: −15–60 % and −25–85 % towards the mid and end-21st century in terms of standardized mean, respectively, for the entire French Alps over the different altitudes, slopes and time scales. Corresponding variance ratios also decrease, leading to small (if not zero) probabilities to exceed the reference mean already in 2020–50 (Table 5). With regards to snow precipitations, changes in interannual means are more homogeneous between regions and even elevations. This arises because, even if snow precipitation are better conserved under future climate at 3000 m, warmer temperatures leads to accelerated melting during spring and to a higher snowpack bulk density at all altitudes, leading to smaller corresponding snow depths. It can however be noted that the decrease is slightly more marked for north facing slopes than for south ones, presumably because modified meteorological conditions induce more snowmelt in the future than currently on these slopes. In addition, the reduction of the interannual variability affects south facing slopes much more than north ones, especially at low altitudes, because, for south facing slopes, the annual mean total snow depth is very small for each year of the future simulation, leading to much lower variance, for example, only 1–25 % of the one of the reference period at end-21st century for the entire French Alps over the full year (Table 5).

3.1.4 Wet and ~~fresh~~ snow depths

Regarding thicknesses of wet snow (Fig. 7), at 1800 m, negative differences in interannual means and small variance ratios with regards to the reference period, increased at the end-21st century, are directly linked with the small (often close to zero according to exceedence probabilities) total snow depths expected in future at this elevation (Table 5). In contrast, at high elevation, especially for northern slopes, wet snow amounts are expected to greatly increase with regards to the reference period where they ~~were~~ negligible due to predominant non-melting conditions (sufficient cold temperatures). Similarly to total snow depth, predicted differences are often less important between the mid and end-21st century than between the reference period and the mid-21st century. They can even be less important between the reference period and the end 21st century than between the reference period and the mid-21st century when the warming becomes important enough to preclude very high snow depths even at high elevation. For example, for the entire French Alps, at the annual time scale, for a north facing slope at 3000 m, the interannual mean increase with regards to the reference period is +104 % and +76 % towards the mid and end-21st century, respectively (Table 5). Regional north/south differences are quite small. It can only be noted that the high altitude increase is slightly more marked in the northern French Alps (Fig. 7). In terms of seasonal differences, in addition to the high altitude increase/low altitude decrease visible at the annual scale and generally enhanced for spring season, one can note a moderate low altitude increase ~~in winter~~ for north facing slopes (+27 % and +33 % towards the mid and end-21st century, respectively, Table 5) that ~~where little concerned by wet snow~~ during the reference period.

Finally, following temperature and precipitation phase changes, thicknesses of recent dry snow are projected to decrease in the future, noteworthy already for the mid-21st century with regards to the reference period. At the annual time scale, the −40–50 % and −50–70 % decrease in interannual mean for the mid and end-21st century, respectively, accompanied by a strong reduction of interannual variability, is rather homogenous for the different slopes, elevations, or regions (Fig. 8). This leads to probabilities to exceed reference values in future climate even smaller than for total snow depths (Table 5). As for many other variables, the decrease appears slightly more marked during spring sub-season, with e.g. −10–25 % and −20–35 % for the entire French Alps in winter/spring, respectively for the mid-21st century with regards to the reference period (Table 5).

3.2 Avalanche activity in future

3.2.1 Projections of CI values

The Cramer test indicates that the joint distribution of the variables corresponding to each of the fitted regression model is always significantly different in the two future periods (still under the A1B scenario) from the reference period (p values largely under the 0.05 significance level, Table 8), except for the Northern French Alps in winter. In the latter case, the model has one single covariate (Table 2). Significant differences also exist for most of the joint distributions between the two future periods. These results suggest that avalanche activity, as a combination of different unstationary drivers, may encounter in the future changes even more important than those expected for each of the snow and meteorological variables.

In more details, at the scale of the entire French Alps, obtained CI projections (Fig. 3, Sect. 2), show clear decreases for the full year (−20 % and −25 % in standardized interannual mean for the mid and end-21st century, respectively), enhanced for the spring sub-season (−45 % and −55 % for the mid and end-21st century, respectively). These decreases in interannual means are accompanied by strong decreases in interannual variability (Table 6). Opposite trends are clear during the winter sub-season: marked increases (+30 % and +125 % in standardized interannual mean for the mid and end-21st century, respectively), strongly driven by dramatic increases of the interannual variability. These results are well illustrated by exceedence probabilities: at the annual scale and during spring, the probability for a future winter to show an avalanche activity as high as the reference mean is close to zero already for mid 21st century. In contrast, few years with a winter avalanche activity much higher than during the reference period are expected in the future. Indeed, the probabilities for the avalanche activity index in winter to exceed the 95 percentile of the reference period are as high as 0.44 and 0.7 for the mid and end-21st century, respectively (Table 6).

These results are direct consequences of the combined evolution of snow and meteorological variables. Whereas precipitation remain rather stationary, temperature in-

crease interacting with topography controls the amount of snow precipitation and snowpack characteristics all over the avalanche year. Overall, the snow precipitation and depth decrease in mean and variance (Figs. 5 and 6), reducing avalanche activity, especially in spring during which changes in snow variables and even temperatures are particularly strong. On the other hand, more important amounts of wet snow appear earlier in the season, eventually increasing avalanche activity at that time with regards to the reference period, at least for certain years (strong increase of the interannual variability in winter). As for the snow and meteorological variables, it is noticeable that most of the forecasted changes are already important for the mid-21st century. They go on until the end-21st century, but apparently at a slightly lower pace.

Figure 9 shows the CI reference distributions and projections for both sub-regions and the different considered temporal scales. It suggests that the overall decrease in avalanche activity forecasted in terms of the CI for the mid-21st century is mostly driven by a strong decrease in the Northern French Alps during spring, where the decrease is the strongest (−63 %, Table 6), whereas a slight decrease is also predicted in winter sub-season (−21 %), contrary to what is expected at the entire French Alps scale. On the contrary, for the Southern Alps, the spring distribution is thinner than for the reference period, but with a decrease less marked than at the entire Alps scale (−29 %). More dramatically, the winter increase in mean and variance is rather spectacular.

These distinguished north/south pictures may be attributable to altitudinal effects. The southern massifs have a mean altitude higher than the northern ones, whereas the snow and meteorological variable analysis has shown that, at constant altitude, latitudinal gradients have little effects on projected changes. Hence, in the northern massifs, avalanche activity is reduced under climate warming by weaker snow precipitations and snow depths during the full year and even in winter. On the contrary, in the southern massifs, wetting induced by warmer conditions of the still important high altitude snowpack in winter leads to more wet snow (Fig. 7) and therefore more wet snow avalanches in addition to the always possible dry snow releases (at high altitude, dry snow depths remain significant, Fig. 8). Hence, the refined altitudinal control with

distinguished effects at different altitudes on north/south facing slopes that has been highlighted for snowpack variables clearly impacts avalanche activity projections. Note, however, that we cannot refine results as much as for the snow variables, by e.g. analyzing north/south behaviors at fixed altitudes and expositions, because avalanche activity indexes are computed as integrated quantities over massifs and then regions.

Between the 2020–2050 and 2070–2100 periods, the decreasing trends remain the same for the Northern Alps, again more markedly in spring. On the other hand, the overall annual activity is found to stabilize for the Southern Alps (−3 % in interannual mean change between the two periods), whereas the winter increase with regards to the reference period is becoming less important. This is probably because, at the end-21st century, as shown before, the warming is becoming marked enough to significantly reduce the snowpack (and for instance the dry snow pack), even at high altitude in winter.

3.2.2 Comparison of the projected Composite Index and MEPRA Index

The CI projections are worth being compared with future annual/seasonal means of the computed MI (Table 7 and Figs. 10 and 11). At the entire Alps and full year scale, trends are similar: both indexes decrease for future periods, meaning a decrease of the overall avalanche activity. However, this decrease is more important for the CI between the reference period and the mid-21st century, whereas the MI decreases notably only between the mid and the end-21st century (−8 % and −31 % in standardized interannual mean with regards to the reference period for the mid and end-21st century, respectively). Furthermore, the relatively high interannual variability still characterizing the MI in future climate leads to the fact that the probabilities to exceed the mean of the reference period remain, even if they decrease, more significant than predicted by the CI (Table 7). Hence, the MI seems to be able to detect "intense" avalanche years for future periods, whereas the CI forecasts a smoother decreasing trend. For the winter sub-season (Fig. 10), as discussed before, the CI significantly increases in future, but with a strong interannual variability. On the other hand, the MI indicates little changes,

probably due to compensation between an increase of melting snow avalanches due to wetter snowpack, and (i) fewer snow precipitations leading to a thinner snowpack and fewer dry snow avalanches, and (ii) higher temperatures leading to a more intense snow metamorphism earlier in the season leading to a reduced level of instability. During spring, as for the annual scale, while the CI strongly decreases for both future periods in mean and variance, the MI only decreases significantly in mean at the end-21st century whereas, for the mid-21st century, projections show a higher interannual variability.

Regarding sub-regions, the main difference with the CI is that the MI decreases more strongly for the Southern French Alps at annual and spring time scales, and decreases also in winter while the projected CI values show an increase of avalanche activity. This may indicate that the MI is more sensitive to the expected higher temperatures and the subsequent strong decrease of snow precipitation (Figs. 3 and 4), whereas the stepwise selection procedure has picked up only snowpack variables for the CI in this southern region (Table 3) which are less affected due to the high altitude of the massifs, or even destabilized earlier in season by warming as discussed Sect. 3.2.1. On the contrary, for the Northern French Alps, the decrease forecasted by the MI is less strong than predicted by the CI, especially for the mid-century.

Scatter plots for the different regions and seasons between both normalized indexes in future periods (Fig. 11) show that, even if certain local differences obviously exist and the amplitude of the forecasted changes differ, both index are globally coherent: overall, future years with a high MI correspond to the ones with a high CI, and vice versa. This suggests that the overall picture of a decreasing avalanche activity at the largest spatio-temporal scale is rather robust. On the other hand, results obtained at smaller scales may well be more uncertain, for instance those concerning the Southern French Alps for 2020–2050 and the Northern French Alps for the end-21st century for which the determination coefficient between the two indexes is very poor.

3.2.3 Sensitivity to SRES scenarios

The results obtained under A1B scenario were confronted to those corresponding to B1 and A2 scenarios (IPCC, 2007) and are shown Fig. 12. The plotted distributions concern the whole Alps scale, for the full year and the two sub-seasons. All of them show the decrease more marked during spring and less clear during winter discussed previously. Similarly, the increased dispersion of the distributions during winter exists for all the considered scenarios. Hence, with regards to the net changes that can be seen between the reference (in blue) and the two future periods (mid and end-21st century, respectively in green and red), the CI projections seem little sensitive to the selected scenario, especially for the mid-21st century. It can nevertheless be noted that, for the 2070–2100 period, the scenario B1 (the more optimistic one) suggests weaker decreases, with distributions closer to the mid-21st century ones, for all seasons, whereas A2, the most pessimistic scenario, shows logically slightly enhanced decreases. Hence, interestingly, current climate policies may well have (slight) consequences on snow stability one century later.

4 Discussion, conclusion and outlooks

This study has proposed a detailed investigation of changes to be expected for the mid and end-21st century in snowpack variables and avalanche activity under climate warming in the French Alps, which is an area particularly sensitive in terms of avalanche hazard, and, more generally, where socio-economic impacts of snow conditions are considerable. Using downscaled and debiased simulations of a regional climate model feeding a detailed snow cover model, which remains a rather new approach in a mountainous environment, and coupling them with a high-quality and long-term observational avalanche record, we have derived fundamental results for this mountain environment, its economy and ecology in terms of changes anticipation and risk management. Indeed, ~~if~~ forecasting ~~that~~ temperature increase and ~~the~~ associated

snow cover decrease ~~should be expected~~ is not revolutionary, the results obtained for different complex snow variables (e.g. fresh and wet snow depths) are very refined with regards to the state of the art, especially in terms of latitudinal, altitudinal and seasonal gradients. Furthermore, as a continuation of Martin et al. (2001) that initiated future simulations of avalanche activity, they may well be the first future projections based on a combination of climate and land surface modeling in mountainous environment combined to avalanche observations used to infer their links with snow and meteorological conditions. The rigor of the statistical analyzes (significance tests for marginal and joint distributions, etc.) and the usefulness of the indicators they provide (exceedence probabilities, variance ratios, etc.) constitute a rich and robust framework for the analysis of the obtained results.

While precipitations are expected to remain quite stationary (or at least with changes that could not be detected), temperature increase interacting with topography will control the amount of snow precipitation and snowpack characteristics, for instance the rate of decrease of total and dry snow depths. In first approximation, latitude effects are globally of little importance with regards to interannual variability. Hence, at constant altitude, the Southern French Alps are not significantly more affected than the Northern French Alps in terms of snow depth decrease, which is a somewhat unexpected result.

As a general picture, four major points are anticipated to take place over the next decades due to climate change: (i) the appearance of a wet snowpack at high elevations, even in the core of the winter sub-season, (ii) more marked changes during spring sub-season with regards to winter sub-season, (iii) stronger changes for the end-21st century, but already (very) important for the mid-century compared to the reference 1961–1990 period, and (iv) a strong altitudinal control of changes (e.g. snow cover decrease affects low altitudes much more strongly). As a consequence of the latter point, different processes will presumably generate complex evolutions. For example, in winter, at high altitude, wet snow depths are first expected to increase (they were close to zero during the reference period), and then to decrease again when the warming will be important enough to impeach the formation of very deep snow packs.

Concerning the future projections of the composite index of avalanche activity, our main result is a projected general decrease in mean and interannual variability. Therefore, probabilities for future seasons to be as intense as the harsh winters of the reference period are very small, for instance by comparison to changes in snow and meteorological variables which seems less dramatic. The explanation is that avalanche activity changes result from changes in different snow variables which may intensify the response to the climatic signal as suggested by the very strong non stationarities detected in the joint distributions corresponding to most of the modeled composite indexes.

In more details, this expected decrease is amplified in spring sub-season with regards to the full winter, and in the Northern French Alps with regards to the Southern French Alps. A rather strong increase of avalanche activity in terms of interannual mean and, even more, in terms of interannual variability is even expected in winter, for instance in the higher altitude massifs of the Southern French Alps. These distinguished evolutions are mainly related to elevation effects on snow variables in a warming climate: during the 21st century, spring snowpack and the related avalanche activity are found to progressively disappear from low to high altitudes. In addition, winter snowpack will show more and more variability, with possible wetting at increasingly high altitudes, making earlier wet snow avalanches triggers possible in addition to still possible winter dry snow avalanche cycles, eventually increasing avalanche activity at that time, at least as long as a minimal snow cover will be preserved. This picture seems in good agreement with the results of Lavigne et al. (2013) suggesting that increased avalanche activity has already taken place in the high altitude villages of the French Alps.

Most of these changes in snow and avalanche variables are strong for the end-21st century. Noteworthy again, they are already more important than expected for the end of the mid-century, compared with the 1960–1990 period, probably because the latter was relatively cold and snowy, as identified by winter climatologies of the French Alps (Durand et al., 2009b). Time series analysis have also showed relatively

more intense avalanche activity (Eckert et al., 2013) and even short glacial advances (Thibert et al., 2013) during this reference period. In contrast, an accelerated warming has already occurred between 1985 and 2000 (e.g. Beniston, 2005a). Hence, it is very likely that the important changes assessed with regards to the mean 1960–1990 have largely already occurred yet. Some changes may also well slow down between mid and end-21st century because of contradictory effects and compensations such as wet snow depth increase and decrease when warming goes on. Finally, forecasted changes at mid-21st century do not seem to be influenced by the choice of the climatic IPCC (2007) SRES scenario, since just a slight differentiation between three rather different scenarios is visible at the end-21st century. This apparent robustness has to be confirmed by the new more accurate scenarios that have just been published (IPCC, 2013).

Beyond these general findings, numerous uncertainty sources must be kept in mind while considering our results. Those related to snow and meteorological simulations and future forecasts in mountainous environment are detailed in Rousselot et al. (2012), while those specifically linked to the composite index and the linear regression approach are discussed in Castebrunet et al. (2012). However, a specific difficulty is worth to be discussed which arises from the combination of all these approaches in this paper. Indeed, it must be remembered that our regression models remain linear which is arguably an oversimplified approximation of the true relationship between avalanche activity and snow and meteorological conditions under the reference climate. Despite the fact that the cross-validation is very conclusive (an encouraging but mandatory requirement), since the real avalanche-climate is, in reality, much more complex and clearly nonlinear, whether or not these regression models can be trusted to assess avalanche activity under future changed climate remains questionable. Our feeling is that, in first approximation, the answer is yes, since our statistical regression models seem able to adequately reproduce different avalanche triggering contexts, capturing elevation and latitudes effects in a rather intuitive (and hopefully realistic) way. Hence, they may well, by picking up a few meaningful variables, capture the

predominant physical processes relating avalanche to snowpack variables at each considered spatio-temporal scale, as suggested by the robustness of the cross-validation results.

The comparison with the MI, readily available in future period from the projection of snow and meteorological conditions, can be seen as a way of confirming (or not) the projections in terms of CI. Overall, the CI and MI see rather similar decreasing trends, and scatter plots (Fig. 11) have shown that they see the same relative high/low activity in future years. Some differences have however been highlighted: with the MI, a later reaction to changes (significantly at the end of the 21st century only), a lower shrinkage of the highest values, and regional/seasonal differences such as the absence of winter increase in the southern massifs, clear with the CI. These divergences are strong reasons to consider detailed projections with care and presumably undertake further work to better understand and refine them. They were however clearly expectable given the rather different ways future avalanche activity is assessed in the future with the CI and through the MI. For instance, ith regards to the CI, the MI may better take into account the reduction of snow extensions under warming and the "true" avalanche–climate relationship. On the other hand, it is not based on real observed activity, and if it well describes intense avalanche activity during cold winter periods, it is less well suited to represent sporadic snow melting triggering as discussed in Castebrunet et al. (2012). The latter argument is the main reason for which we based our work mainly on the CI, since a warming climate is anticipated to favor such events. Nevertheless, since the MI captures well the harsh "full winter" conditions, projections concerning the evolution of the winters with the highest activity may well be more realistic than the ones of the CI on this point. Hence, probabilities of exceeding high values characteristic of the reference period may well decrease during the 21st century, but presumably not as strong and fast as predicted by the CI, an important point in a risk assessment perspective.

Finally, it is worth noting that the threshold values and exceedence probabilities we assessed for reference and future periods do not ~~here~~ represent extreme avalanche cycles but (sub) seasons characterized by the strongest avalanche activity. More gen-

erally, this study has been realized with large scale data, which involved snowpack characteristics and avalanche trigger numbers averaged/cumulated over long periods and large areas. To better apprehend avalanche risk in future, we therefore call for further analysis of future changes in (i) small spatial (path) scale intensity variables such as runout distances and pressures relevant for urbanism and road viability and their link to snow and meteorological variables through e.g. friction parameters (Naaim et al., 2013), (ii) short time scales intense avalanche cycles threatening mountain practitioners, as done with the MI in Giraud et al. (2013). These are however more complicated problems as they involve (i) avalanche propagation and in particular its constraint by each site-specific topography and, (ii) a specific extreme value statistical framework.

Acknowledgements. This work was mainly done in the framework of the joint Météo France–Irstea ECANA project (http://www.avalanches.fr/projet-ecana/) funded by the French Ministry of the Environment (Risk Division-DGPR). It has also benefited from the results of the ANR SCAMPEI project (http://www.cnrm.meteo.fr/scampei/presentation_scampei/).

References

Ammann, W. and Bebi, P.: Der Lawinenwinter 1999, Ereignisanalyse, SLF Davos Bibliothek, 588 pp., 2000.

Ancey, C., Gervasoni, C., and Meunier, M.: Computing extreme avalanches, Cold Reg. Sci. Technol., 39, 161–184, 2004.

Bavay, M., Lehning, M., Jonas, T., and Loewe, H.: Simulations of future snow cover and discharge in Alpine headwaters catchments, Hydrol. Process., 23, 95–108, 2009.

Beniston, M.: Variations of snow depth and duration in the Swiss Alps over the last 50 years: links to changes in large-scale climatic forcings, Climatic Change, 3, 281–300, 1997.

Beniston, M.: Climatic change in mountain regions: a review of possible impacts, Climatic Change, 59, 5–31, 2003.

Beniston, M.: Warm winter spells in the Swiss Alps: strong heat waves in a cold season?, Geophys. Res. Lett., 32, L01812, doi:10.1029/2004GL021478, 2005a.

Beniston, M.: Mountain climates and climatic change: an overview of processes focusing on the European Alps, Pure Appl. Geophys., 162, 1587–1606, 2005b.

Beniston, M., Keller, F., and Goyette, S.: Snow pack in the Swiss Alps under changing climatic conditions: an empirical approach for climate impacts studies, Theor. Appl. Climatol., 74, 19–31, 2003.
Brown, R. D.: Northern Hemisphere snow cover variability and change, 1915–97, J. Climate, 13, 2339–2355, 2000.
Caussinus, H. and Mestre, O.: Detection and correction of artificial shifts in climate series, Appl. Stat.-J. Roy. St. C, 53, 405–425, 2004.
Castebrunet, H., Eckert, N., and Giraud, G.: Snow and weather climatic control on snow avalanche occurrence fluctuations over 50 yr in the French Alps, Clim. Past, 8, 855–875, doi:10.5194/cp-8-855-2012, 2012.
Déqué, M.: Frequency of precipitation and temperature extremes over France in an anthropogenic scenario: model results and statistical correction according to observed values, Global Planet. Change, 57, 16–26, doi:10.1016/j.gloplacha.2006.11.030, 2007.
Déqué, M. and Somot, S.: Variable resolution versus limited area modelling: perfect model approach, Research Activities on Atmospheric and Oceanic Modeling, 37, 3.03–3.04, 2007.
Dumas, D.: Changes in temperature and temperature gradients in the French Northern Alps during the last century, Theor. Appl. Climatol., 111, 223–233, doi:10.1007/s00704-012-0659-1, 2012.
Durand, Y., Giraud, G., Brun, E., Mérindol, L., and Martin, E.: A computer-based system simulating snowpack structures as a tool for regional avalanche forecasting, J. Glaciol., 45, 469–484, 1999.
Durand, Y., Laternser, M., Giraud, G., Etchevers, P., Lesaffre, L., and Mérindol, L.: Reanalysis of 44 yr of climate in the French Alps (1958–2002): methodology, model validation, climatology, and trends for air temperature and precipitation, J. Appl. Meteorol. Clim., 48, 29–449, 2009a.
Durand, Y., Laternser, M., Giraud, G., Etchevers, P., Mérindol, L., and Lesaffre, B.: Reanalysis of 47 yr of climate in the French Alps (1958–2005): climatology and trends for snow cover, J. Appl. Meteorol. Clim., 48, 2487–2512, 2009b.
Eckert, N., Parent, E., and Richard, D.: Revisiting statistical–topographical methods for avalanche predetermination: Bayesian modelling for runout distance predictive distribution, Cold Reg. Sci. Technol., 49, 88–107, 2007a.
Eckert, N., Parent, E., Belanger, L., Garcia, S.: Hierarchical modelling for spatial analysis of the number of avalanche occurrences at the scale of the township, Cold Reg. Sci. Technol., 50, 97–112, 2007b.

Eckert, N., Parent, E., Faug, T., and Naaim, M.: Bayesian optimal design of an avalanche dam using a multivariate numerical avalanche model, Stoch. Env. Res. Risk. A., 23, 1123–1141, 2009.
Eckert, N., Parent, E., Kies, R., and Baya, H.: A spatio-temporal modelling framework for assessing the fluctuations of avalanche occurrence resulting from climate change: application to 60 years of data in the northern French Alps, Climatic Change, 101, 515–553, 2010a.
Eckert, N., Baya, H., and Deschâtres, M.: Assessing the response of snow avalanche runout altitudes to climate fluctuations using hierarchical modelling: application to 61 winters of data in France, J. Climate, 23, 3157–3180, 2010b.
Eckert, N., Coleou, C., Castebrunet, H., Giraud, G., Deschatres, M., and Gaume, J.: Cross-comparison of meteorological and avalanche data for characterising avalanche cycles: the example of December 2008 in the eastern part of the French Alps, Cold Reg. Sci. Technol., 64, 119–136, 2010c.
Eckert, N., Keylock, C. J., Castebrunet, H., Lavigne. A., and Naaim, M.: Temporal trends in avalanche activity in the French Alps and subregions: from occurrences and runout altitudes to unsteady return periods, J. Glaciol., 59, 93–114, 2013.
Elsasser, H. and Buerki, R.: Climate change as a threat to tourism in the Alps, Clim. Res., 20, 253–257, 2002.
Falarz, M.: Long-term variability in reconstructed and observed snow cover over the last 100 winter seasons in Cracow and Zakopane (Southern Poland), Clim. Res., 19, 247–256, 2002.
Falarz, M.: Variability and trends in the duration and depth of snow cover in Poland in the 20th century, Int. J. Climatol., 24, 1713–1727, 2004.
Gaume, J., Eckert, N., Chambon, G., Eckert, N., Naaim, M., and Bel, L.: Mapping extreme snowfalls in the French Alps using Max–Stable processes, Water Resour. Res., 49, 1079–1098, 2013.
Giraud, G.: MEPRA: an expert system for avalanche risk forecasting, in: ISSW Proc., Breckenridge, CO, Breckenridge, Colorado, USA, 4–8 October 1992, 97–104, 2013.
Giraud, G., Rousselot, M., Merindol, L., Dombrowski-Etchevers, I., Durand, Y., Déqué, M., Castebrunet, H., and Eckert, N.: Adaptation of current modeled snow covers and avalanche hazards to future climate according several RCM scenarii: application to French Alps, in: International Snow Science Workshop proceedings, 7–11 October 2013, Grenoble-Chamonix, France, 1194–1200, 2013.

Gonseth, C.: Impact of snow variability on the Swiss winter tourism sector: implications in an era of climate change, Climatic Change, 119, 307–320, 2013.
Huntington, T. G., Hodgkins, G. A., Keim, B. D., and Dudley, R. W.: Changes in the proportion of precipitation occurring as snow in New England (1949–2000), J. Climate, 17, 2626–2636, 2004.
IPCC: Climate Change 2007: the Physical Science Basis, Contribution of working group I to the fourth assessment report of the Intergovernmental Panel on Climate Change, edited by: Solomon, S., Qin, D., Manning, M., Chen, Z., Marquis, M., Averyt, K. B., Tignor, M., and Miller, H. L., Cambridge University Press, Cambridge, UK and New York, NY, USA, 2007.
IPCC: Managing the Risks of Extreme Events and Disasters to Advance Climate Change Adaptation, A Special Report of Working Groups I and II of the Intergovernmental Panel on Climate Change, edited by: Field, C. B., Barros, V., Stocker, T. F., Qin, D., Dokken, D. J., Ebi, K. L., Mastrandrea, M. D., Mach, K. J., Plattner, G.-K., Allen, S. K., Tignor, M., and Midgley, P. M., Cambridge University Press, Cambridge, UK, and New York, NY, USA, 582 pp., 2012.
IPCC: Climate Change 2013: the Physical Science Basis, Final draft, available at: http://www.climatechange2013.org/report/ (last access: November 2013), 2013.
Jamard, A. L., Garcia, S., and Bélanger, V.: L'enquête permanente sur les Avalanches (EPA): statistique descriptive générale des événements et des sites. DESS Ingénierie Mathématique Option Statistique, Université Joseph Fourier, Grenoble, France, 101 pp., available at: http://www.avalanches.fr/ (last access: September 2013), 2002.
Jomelli, V., Delval, C., Grancher, D., Escande, S., Brunstein, D., Hetu, B., Filion, L., and Pech, P.: Probabilistic analysis of recent snow avalanche activity and climate in the French Alps, Cold Reg. Sci. Technol., 47, 180–192, 2007.
Keller, F., Goyette, S., and Beniston, M.: Sensitivity analysis of snow cover to climate change scenarios and their impact on plant habitats in alpine terrain, Climatic Change, 72, 299–319, 2005.
Keiler, M., Knight, J., and Harrison, S.: Climate change and geomorphological hazards in the eastern European Alps, Philos. T. R. Soc. Lond., 368, 2461–2479, 2010.
Laternser, M. and Schneebeli, M.: Long-term snow climate trends of the Swiss Alps (1931–99), Int. J. Climatol., 23, 733–750, 2003.
Lavigne, A., Bel, L., Parent, E., and Eckert, N.: A model for spatio-temporal clustering using multinomial probit regression: application to avalanche counts in the French Alps, Environmetrics, 23, 522–534, 2012.

Lavigne, A., Eckert, N., Bel, L., and Parent, E.: Adding expert contribution to the spatio-temporal modeling of avalanche activity under different climatic influences, J. Roy. Stat. Soc., submitted, 2013.
Lazar, B. and Williams, M.: Climate change in western ski areas: potential changes in the timing of wet avalanches and snow quality for the Aspen ski area in the years 2030 and 2100, Cold Reg. Sci. Technol., 51, 219–228, 2008.
López-Moreno, J. I., Goyette, S., and Beniston, M.: Impact of climate change on snowpack in the Pyrenees: horizontal spatial variability and vertical gradients, J. Hydrol., 374, 384–396, 2009.
López-Moreno, J. I., Goyette, S., Vicente-Serrano, S. M., and Beniston, M.: Effects of climate change on the intensity and frequency of heavy snowfall events in the Pyrenees, Climatic Change, 105, 489–508, 2011.
Martin, E., Brun, E., and Durand, Y.: Sensitivity of the French Alps snow cover to the variation of climatic variables, Ann. Geophys., 12, 469–477, doi:10.1007/s00585-994-0469-6, 1994.
Martin, E., Giraud, G., Lejeune, Y., and Boudart, G.: Impact of climate change on avalanche hazard, Ann. Glaciol., 32, 163–167, 2001.
McCabe, G. J. and Wolock, D. M.: Long-term variability in Northern Hemisphere snow cover and associations with warmer winters, Climatic Change, 99, 141–153, 2010.
Mitterer, C., Hirashima, H., and Schweizer, J.: Wet-snow instabilities: comparison of measured and modelled liquid water content and snow stratigraphy, Ann. Glaciol., 52, 201–208, 2011.
Morán-Tejeda, E., López-Moreno, J. I., and Beniston, M.: The changing roles of temperature and precipitation on snowpack variability in Switzerland as a function of altitude, Geophys. Res. Lett., 40, 2131–2136, doi:10.1002/grl.50463, 2013.
Mote, P. W.: Trends in snow water equivalent in the Pacific Northwest and their climatic causes, Geophys. Res. Lett., 30, 1601, doi:10.1029/2003GL017258, 2003.
Mougin, P.: Les avalanches en Savoie. Ministère de l'Agriculture, Direction Générale des Eaux et Forêts, Service des Grandes Forces Hydrauliques, Paris, Tech. Rep., 175–317, 1922.
Naaim, M., Durand, Y., Eckert, N., and Chambon, G.: Dense avalanche friction coefficients: influence of physical properties of snow, J. Glaciol., 59, 771–782, 2013.
ONERC: Changements climatiques dans les Alpes: impacs et risques naturels, Rapport technique no. 1, 86 pp., available at: http://www.risknat.org/docs/Technical%20Report%20N%B01.pdf (last access: November 2013), 2008.
Räisänen, J.: Warmer climate: less or more snow?, Clim. Dynam., 30, 307–319, 2008.

Rangwala, I. and Miller, J. R.: Climate change in mountains: a review of elevation-dependent warming and its possible causes, Climatic Change, 114, 527–547, 2012.

Richard, D., Marcepoil, E., and Boudières, V.: Changement climatique et développement des territoires de montagne: quelles connaissances pour quelles pistes d'action?, Website Rev. Geogr.Alp., http://rga.revues.org/index1322.html (last access: November 2013), 2010.

Rousselot, M., Durand, Y., Giraud, G., Mérindol, L., Dombrowski-Etchevers, I., Déqué, M., and Castebrunet, H.: Statistical adaptation of ALADIN RCM outputs over the French Alps – application to future climate and snow cover, The Cryosphere, 6, 785–805, doi:10.5194/tc-6-785-2012, 2012.

Saporta, G.: Probabilités, Analyse des Données et Statistique, Technip, 2nd edn., Broché, Paris, France, 622 pp., 2006.

Thibert, E., Eckert, N., and Vincent, C.: Climatic drivers of seasonal glacier mass balances: an analysis of 6 decades at Glacier de Sarennes (French Alps), The Cryosphere, 7, 47–66, doi:10.5194/tc-7-47-2013, 2013.

Uppala, S., Kallberg, P. W., Hernandez, A., Saarinen, S., Fiorino, M., Li, X., Onogi, K., Sokka, N., Andrae, U., and Da Costa Bechtold, V.: ECMWF, "ERA-40: ECMWF 45 yr reanalysis of the global atmosphere and surface conditions 1957–2002", ECMWF Newsletter, No. 101, ECMWF, Reading, UK, 2–21, 2004.

Valt, M. and Cianfarra, P.: Recent snow cover variability in the Italian Alps, Cold Reg. Sci. Technol., 64, 146–157, 2010.

Wilby, R. L., Wigley, T. M. L., Conway, D., Jones, P. D., Hewitson, B. C., Main, J., and Wilks, D. S.: Statistical downscaling of generalcirculation model output: a comparison of methods, Water Resour. Res., 34, 2995–3008, 1998.

Table 1. Regression models characteristics for the French Alps (all year, winter and spring periods). For each model, the different variables are those selected by the stepwise regression. For each retained normalized explanatory variables X_{jt}^{norm}, β_j is the corresponding weighting coefficient in the model, ρ_j the correlation coefficient between X_{jt}^{norm}. β_j and the composite index, and R^2 the determination coefficient of the model.

Explanatory variables j	β_j	ρ_j	R^2
French Alps, year			
Snow precipitation (1800 m)	0.09	0.84	0.91
Thickness of wet snow (1800 m, north)	0.06	0.84	
Snow depth (2400 m, north)	−0.13	−0.70	
Thickness of surface recent dry snow (3000 m, north)	0.12	0.89	
French Alps, winter			
Thickness of wet snow (2400 m, north)	0.09	0.23	0.82
Thickness of surface recent dry snow (3000 m, east)	0.34	0.85	
Thickness of surface recent dry snow (2400 m, west)	−0.19	−0.80	
French Alps, spring			
Thickness of wet snow (2400 m, north)	−0.09	0.01	0.89
Thickness of wet snow (2400 m, east)	0.16	0.53	
Thickness of surface recent dry snow (3000 m, south)	−0.13	−0.73	
Thickness of surface recent dry snow (2400 m, west)	0.26	0.81	
Snow depth (3000 m, west)	−0.07	−0.45	

Table 2. Regression models characteristics for the Northern French Alps (all year, winter and spring periods). For each retained explanatory variables X_{jt}^{norm}, β_j is the corresponding weighting coefficient in the model, ρ_j the correlation coefficient between X_{jt}^{norm}. β_j and the composite index, and R^2 the determination coefficient of the model.

Explanatory variables j	β_j	ρ_j	R^2
Northern French Alps, year			
Tmax (2400 m)	−0.15	0.32	0.97
Tmax (3000 m)	0.19	−0.19	
Thickness of wet snow (1800 m, north)	−0.05	−0.85	
Thickness of surface recent dry snow (1800 m, north)	0.43	0.87	
Thickness of surface recent dry snow (3000 m, north)	−0.27	−0.90	
Thickness of wet snow (2400 m, east)	0.17	0.61	
Thickness of surface recent dry snow (3000 m, east)	0.43	0.90	
Thickness of surface recent dry snow (1800 m, west)	−0.34	−0.87	
Thickness of wet snow (2400 m, west)	−0.11	−0.50	
Northern French Alps, winter			
Thickness of surface recent dry snow (3000 m, east)	0.22	0.85	0.71
Northern French Alps, spring			
Thickness of surface recent dry snow (2400 m, north)	0.35	0.78	0.80
Thickness of wet snow (2400 m, east)	0.26	0.45	
Thickness of wet snow (2400 m, west)	−0.20	−0.33	
Thickness of surface recent dry snow (3000 m, west)	−0.21	−0.72	

Table 3. Regression models characteristics for the Southern French Alps (all year, winter and spring periods). For each retained explanatory variables X_{jt}^{norm}, β_j is the corresponding weighting coefficient in the model, ρ_j the correlation coefficient between X_{jt}^{norm}. β_j and the composite index, and R^2 the determination coefficient of the model.

Explanatory variables j	β_j	ρ_j	R^2
Southern French Alps, year			
Snow precipitation (3000 m)	−0.08	−0.55	0.91
Thickness of wet snow (1800 m, north)	0.14	0.86	
Snow depth (2400 m, north)	−0.09	−0.65	
Thickness of surface recent dry snow (3000 m, west)	0.22	0.85	
Southern French Alps, winter			
Thickness of wet snow (2400 m, north)	0.11	0.23	0.86
Thickness of surface recent dry snow (2400 m, east)	−0.20	−0.80	
Thickness of surface recent dry snow (3000 m, west)	0.39	0.87	
Southern French Alps, spring			
Thickness of surface recent dry snow (2400 m, east)	0.13	0.83	0.77
Snow depth (1800 m, south)	0.08	0.71	

Table 4. Predictive performance of CI regression models in cross validation, with each year included or not in the calibration sample. The success rate corresponds to the percentage of prediction falling into the 95 % confidence interval around the data.

	Prediction success rate (%), calibration	Prediction success rate (%), validation
French Alps, whole year	93	90
French Alps, winter	97	93
French Alps, spring	97	93
Northern French Alps, whole year	93	87
Northern French Alps, winter	97	87
Northern French Alps, spring	93	93
Southern French Alps, whole year	97	90
Southern French Alps, winter	93	93
Southern French Alps, spring	97	93

Table 5. Changes in meteorological and snow variables between the reference period and the two future periods, for the entire French Alps, during the whole year, the winter and the spring periods. Ref, 2020–2050 and 2070–2100 correspond to the three considered periods: reference (1960–1990), mid and end of the 21st century, respectively. The probability for a future year to be higher than the reference mean and the 75 and 95 % percentiles of the reference distribution is quantified, as well as ratios and differences between the reference variance/mean and the two future variances/means, respectively. For the Kolmogorov–Smirnov test, bold values indicate different samples at the 0.05 significance level. When the null hypothesis of similar underlying distributions is not rejected, exceedence probabilities appear in italic, as differences with the reference period may be insignificant. When the assumption of a Gaussian distribution is rejected for at least one of the considered samples, the significance of the variance comparison cannot be tested so that the variance ratios appear in italic. When the assumption of Gaussian distributions with similar variances is rejected for at least one of the considered samples, the significance of the mean comparison cannot be tested so that the mean standardized difference appears in italic. When the significance of variance/mean comparisons could be tested, ratios/standardized differences rejecting the null hypothesis of equality are shown in bold.

Table 5. Continued.

Whole year	Distribution comparison (p value, Kolmogorov–Smirnov test)			Probability mean(2020–2050)>			Probability mean(2070–2100)>			Means comparison (standardized differences)			Variance comparison (ratios)		
	ref/2020–2050	ref/2070–2100	2020–2050/2070–2100	mean(ref)	q75(ref)	q95(ref)	mean(ref)	q75(ref)	q95(ref)	2020/2050–ref	2070/2100–ref	2070/2100–2020/2050	2020/2050–ref	2070/2100–ref	2070/2100–2020/2050
Tmin 1800 m	**0.00**	**0.00**	**0.00**	1	1	0.75	1.00	1.00	1.00	*0.76*	1.53	*0.77*	*0.99*	0.85	*0.86*
Tmax 1800 m	**0.00**	**0.00**	**0.00**	0.99	0.94	0.54	1.00	1.00	1.00	**0.61**	**1.29**	**0.68**	1.03	0.95	0.92
Tmin 3000 m	**0.00**	**0.00**	**0.00**	1.00	0.99	0.91	1.00	1.00	1.00	**0.66**	**1.33**	**0.67**	0.95	0.95	1.01
Tmax 3000 m	**0.00**	**0.00**	**0.00**	0.99	0.96	0.59	1.00	1.00	1.00	**0.57**	**1.15**	**0.59**	1.01	0.88	0.86
Ptot 1800 m	0.76	0.25	0.65	*0.43*	*0.21*	*0.01*	*0.28*	*0.10*	*0.00*	−0.04	*−0.14*	*−0.09*	0.90	*0.79*	*0.87*
SP 1800 m	**0.00**	**0.00**	**0.00**	0.07	0.01	0.00	0.00	0.00	0.00	**−0.28**	*−0.51*	**−0.23**	0.66	**0.39**	0.59
Ptot 3000 m	0.94	0.14	0.41	0.41	0.20	0.01	0.26	0.09	0.00	−0.05	**−0.13**	−0.08	0.88	0.77	0.87
SP 3000 m	**0.03**	**0.00**	**0.01**	0.21	0.08	0.01	0.03	0.00	0.00	**−0.15**	**−0.33**	**−0.17**	0.77	0.58	0.75
SD (1800 m,north)	**0.00**	**0.00**	**0.00**	0.00	0.00	0.00	0.00	0.00	0.00	*−0.52*	*−0.65*	*−0.14*	**0.16**	**0.05**	**0.30**
SD (3000 m, north)	**0.00**	**0.00**	**0.00**	0.00	0.00	0.00	0.00	0.00	0.00	*−0.63*	*−0.83*	**−0.21**	**0.46**	**0.32**	0.68
SD (1800 m, south)	**0.00**	**0.00**	**0.00**	0.00	0.00	0.00	0.00	0.00	0.00	*−0.32*	*−0.38*	*−0.07*	*0.08*	*0.01*	*0.16*
SD (3000 m, south)	**0.00**	**0.00**	**0.04**	0.01	0.00	0.00	0.00	0.00	0.00	*−0.39*	*−0.51*	**−0.12**	**0.39**	**0.25**	0.63
TWS (1800 m, north)	**0.00**	**0.00**	**0.00**	0.00	0.00	0.00	0.00	0.00	0.00	*−0.41*	*−0.56*	−0.14	**0.25**	**0.11**	0.44
TWS (3000 m, north)	**0.00**	**0.00**	**0.01**	1.00	1.00	0.93	0.99	0.99	0.84	*1.04*	*0.76*	**−0.28**	*3.39*	*2.26*	0.67
TWS (1800 m, south)	**0.00**	**0.00**	**0.00**	0.01	0.00	0.00	0.00	0.00	0.00	*−0.30*	*−0.39*	*−0.08*	*0.16*	*0.03*	*0.21*
TWS (3000 m, south)	**0.01**	0.84	**0.02**	0.77	0.57	0.25	*0.54*	*0.27*	*0.04*	**0.21**	0.02	**−0.19**	1.55	0.97	0.62
TSRDS (1800 m, north)	**0.00**	**0.00**	**0.00**	0.00	0.00	0.00	0.00	0.00	0.00	*−0.49*	*−0.60*	*−0.11*	**0.12**	**0.04**	**0.36**
TSRDS (3000 m, north)	**0.00**	**0.00**	**0.00**	0.00	0.00	0.00	0.00	0.00	0.00	*−0.52*	*−0.67*	**−0.14**	**0.26**	**0.15**	0.57
TSRDS (1800 m, south)	**0.00**	**0.00**	**0.00**	0.00	0.00	0.00	0.00	0.00	0.00	*−0.44*	*−0.54*	*−0.10*	**0.12**	**0.04**	**0.37**
TSRDS (3000 m, south)	**0.00**	**0.00**	**0.03**	0.00	0.00	0.00	0.00	0.00	0.00	*−0.44*	*−0.57*	**−0.13**	**0.25**	**0.14**	0.58

Table 5. Continued.

Winter	Distribution comparison (p value, Kolmogorov–Smirnov test)			Probability mean(2020–2050)>			Probability mean(2070–2100)>			Means comparison (standardized differences)			Variance comparison (ratios)		
	ref/2020–2050	ref/2070–2100	2020–2050/2070–2100	mean(ref)	q75(ref)	q95(ref)	mean(ref)	q75(ref)	q95(ref)	2020/2050–ref	2070/2100–ref	2070/2100–2020/2050	2020/2050–ref	2070/2100–ref	2070/2100–2020/2050
Tmin 1800 m	**0.00**	**0.00**	**0.01**	0.90	0.69	0.30	0.99	0.93	0.68	**0.30**	**0.53**	**0.23**	0.87	0.87	1.00
Tmax 1800 m	**0.00**	**0.00**	**0.00**	0.84	0.74	0.08	0.98	0.95	0.31	**0.20**	**0.38**	**0.18**	1.00	0.91	0.91
Tmin 3000 m	**0.00**	**0.00**	**0.01**	0.87	0.64	0.26	0.98	0.90	0.61	**0.29**	**0.52**	**0.23**	0.90	0.88	0.98
Tmax 3000 m	**0.00**	**0.00**	**0.00**	0.86	0.69	0.12	0.98	0.94	0.40	**0.23**	**0.44**	**0.21**	0.94	0.82	0.87
Ptot 1800 m	1.00	0.96	1.00	*0.47*	*0.19*	*0.07*	*0.46*	*0.18*	*0.06*	−0.02	−0.03	−0.01	0.93	0.92	0.98
SP 1800 m	**0.00**	**0.00**	**0.00**	0.22	0.03	0.01	0.03	0.00	0.00	**−0.17**	*−0.35*	*−0.18*	0.64	*0.44*	*0.69*
Ptot 3000 m	1.00	0.96	1.00	*0.48*	*0.18*	*0.05*	*0.47*	*0.17*	*0.05*	−0.01	−0.02	−0.01	0.93	0.92	0.99
SP 3000 m	1.00	0.96	1.00	*0.48*	*0.18*	*0.05*	*0.45*	*0.16*	*0.04*	-0.02	-0.03	-0.02	0.92	0.88	0.96
SD (1800 m, north)	**0.00**	**0.00**	**0.00**	0.08	0.02	0.00	0.00	0.00	0.00	**−0.25**	*−0.45*	*−0.20*	0.60	**0.25**	**0.42**
SD (3000 m, north)	**0.03**	**0.00**	**0.01**	0.19	0.07	0.00	0.04	0.01	0.00	**−0.20**	**−0.37**	**−0.17**	0.75	0.63	0.84
SD (1800 m, south)	**0.00**	**0.00**	**0.01**	0.10	0.01	0.00	0.00	0.00	0.00	*−0.18*	*−0.30*	*−0.11*	**0.35**	*0.07*	*0.20*
SD (3000 m, south)	0.20	**0.00**	0.26	*0.27*	*0.07*	*0.00*	0.11	0.01	0.00	**−0.15**	**−0.26**	−0.11	0.85	0.67	0.79
TWS (1800 m, north)	**0.01**	**0.00**	0.84	0.66	0.54	0.19	0.76	0.66	0.16	*0.27*	*0.33*	*0.06*	*2.39*	*2.81*	*1.17*
TWS (3000 m, north)	**0.03**	**0.00**	**0.00**	0.44	0.72	0.39	0.76	0.84	0.72	*0.17*	*1.26*	*1.10*	*7.74*	*102.90*	*13.30*
TWS (1800 m, south)	0.76	0.08	**0.02**	*0.39*	*0.16*	*0.07*	*0.19*	*0.06*	*0.00*	*−0.02*	*−0.17*	*−0.15*	*1.25*	*0.36*	*0.29*
TWS (3000 m, south)	0.11	**0.00**	0.15	*0.54*	*0.30*	*0.13*	0.68	0.37	0.10	*0.13*	*0.20*	*0.07*	*2.01*	*2.35*	*1.17*
TSRDS (1800 m, north)	**0.00**	**0.00**	**0.00**	0.07	0.00	0.00	0.00	0.00	0.00	*−0.27*	*−0.44*	*−0.17*	*0.44*	0.15	*0.35*
TSRDS (3000 m, north)	0.20	**0.00**	0.08	*0.29*	*0.06*	*0.01*	0.10	0.01	0.00	−0.12	*−0.23*	−0.11	0.66	**0.43**	0.65
TSRDS (1800 m, south)	**0.00**	**0.00**	**0.00**	0.08	0.00	0.00	0.00	0.00	0.00	*−0.24*	*−0.38*	*−0.15*	**0.38**	**0.14**	**0.38**
TSRDS (3000 m, south)	0.20	**0.04**	0.26	*0.32*	*0.07*	*0.01*	0.16	0.01	0.00	−0.11	*−0.20*	−0.08	0.70	**0.47**	0.68

Table 5. Continued.

Spring	Distribution comparison (p value, Kolmogorov–Smirnov test)			Probability mean(2020–2050)>			Probability mean(2070–2100)>			Means comparison (standardized differences)			Variance comparison (ratios)		
	ref/2020–2050	ref/2070–2100	2020–2050/2070–2100	mean(ref)	q75(ref)	q95(ref)	mean(ref)	q75(ref)	q95(ref)	2020/2050−ref	2070/2100−ref	2070/2100−2020/2050	2020/2050−ref	2070/2100−ref	2070/2100−2020/2050
Tmin 1800 m	**0.00**	**0.00**	**0.00**	0.99	0.96	0.66	1.00	1.00	0.98	**0.50**	**0.86**	**0.36**	0.84	0.92	1.10
Tmax 1800 m	**0.00**	**0.00**	**0.00**	0.97	0.83	0.60	1.00	1.00	0.98	**0.45**	**0.92**	**0.47**	0.86	1.04	1.21
Tmin 3000 m	**0.00**	**0.00**	**0.00**	0.97	0.89	0.58	1.00	0.99	0.94	**0.36**	**0.64**	**0.29**	0.84	0.99	1.17
Tmax 3000 m	**0.00**	**0.00**	**0.00**	0.96	0.89	0.46	1.00	1.00	0.93	**0.36**	**0.73**	**0.36**	0.85	1.00	1.19
Ptot 1800 m	1.00	0.88	0.48	*0.54*	*0.27*	*0.08*	*0.45*	*0.19*	*0.05*	0.02	−0.03	−0.05	1.06	1.01	0.96
SP 1800 m	**0.00**	**0.00**	**0.01**	0.06	0.00	0.00	0.00	0.00	0.00	**−0.31**	*−0.47*	**−0.17**	0.51	**0.26**	0.52
Ptot 3000 m	0.94	0.29	0.46	*0.53*	*0.33*	*0.04*	*0.43*	*0.25*	*0.02*	0.02	−0.03	−0.05	1.04	0.98	0.95
SP 3000 m	0.34	**0.00**	**0.01**	*0.40*	*0.22*	*0.02*	0.12	0.04	0.00	−0.05	**−0.21**	−0.16	0.97	0.70	0.72
SD (1800 m,north)	**0.00**	**0.00**	**0.00**	0.00	0.00	0.00	0.00	0.00	0.00	*−0.39*	*−0.56*	*−0.18*	**0.31**	*0.07*	*0.23*
SD (3000 m, north)	**0.01**	**0.00**	**0.03**	0.18	0.04	0.00	0.03	0.00	0.00	**−0.25**	**−0.54**	**−0.28**	0.96	1.00	1.04
SD (1800 m, south)	**0.00**	**0.00**	**0.00**	0.01	0.00	0.00	0.00	0.00	0.00	*−0.24*	*−0.30*	*−0.06*	*0.09*	*0.01*	*0.09*
SD (3000 m, south)	**0.01**	**0.00**	0.07	0.21	0.05	0.01	0.04	0.00	0.00	**−0.20**	**−0.37**	**−0.17**	0.92	0.67	0.72
TWS (1800 m, north)	**0.00**	**0.00**	**0.00**	0.03	0.00	0.00	0.00	0.00	0.00	*−0.34*	*−0.57*	*−0.23*	**0.43**	*0.11*	*0.25*
TWS (3000 m, north)	**0.00**	**0.00**	0.27	0.97	0.97	0.74	0.99	0.99	0.87	*0.66*	*0.86*	**0.21**	*2.57*	*3.20*	1.25
TWS (1800 m, south)	**0.00**	**0.00**	**0.00**	0.06	0.00	0.00	0.00	0.00	0.00	*−0.25*	*−0.32*	*−0.08*	*0.15*	*0.01*	*0.07*
TWS (3000 m, south)	**0.00**	**0.09**	0.17	0.81	0.65	0.22	0.71	0.54	0.17	**0.26**	**0.18**	−0.08	*1.50*	1.76	*1.17*
TSRDS (1800 m, north)	**0.00**	**0.00**	**0.01**	0.01	0.00	0.00	0.00	0.00	0.00	*−0.33*	*−0.44*	*−0.11*	**0.27**	**0.11**	**0.40**
TSRDS (3000 m, north)	**0.05**	**0.00**	**0.03**	0.15	0.05	0.00	0.01	0.00	0.00	**−0.20**	*−0.35*	**−0.15**	0.54	**0.33**	0.62
TSRDS (1800 m, south)	**0.00**	**0.00**	**0.04**	0.01	0.00	0.00	0.00	0.00	0.00	*−0.34*	*−0.46*	*−0.12*	**0.27**	**0.10**	**0.37**
TSRDS (3000 m, south)	**0.03**	**0.00**	**0.01**	0.16	0.03	0.00	0.01	0.00	0.00	**−0.20**	*−0.36*	**−0.17**	0.51	**0.29**	0.57

T: temperature; Ptot: Total Precipitation; SP: Snow Precipitation; SD: Snow Depth; TWS: Thickness of Wet Snow; TSRDS: Thickness of Surface Recent Dry Snow.

Table 6. Changes in CI models between the reference period and the two future periods. Ref, 2020–2050 and 2070–2100 correspond to the three considered periods: reference (1960–1990), mid and end of the 21st century, respectively. The probability for a future year to be higher than the reference mean and the 75 and 95 % percentiles of the reference distribution is quantified, as well as ratios and differences between the reference variance/mean and the two future variances/means, respectively. For the Kolmogorov–Smirnov test, bold values indicate different samples at the 0.05 significance level. When the null hypothesis of similar underlying distributions is not rejected, exceedence probabilities appear in italic, as differences with the reference period may be insignificant. When the assumption of a Gaussian distribution is rejected for at least one of the considered samples, the significance of the variance comparison cannot be tested so that the variance ratios appear in italic. When the assumption of Gaussian distributions with similar variances is rejected for at least one of the considered samples, the significance of the mean comparison cannot be tested so that the mean standardized difference appears in italic. When the significance of variance/mean comparisons could be tested, ratios/standardized differences rejecting the null hypothesis of equality are shown in bold.

	Distribution comparison (p value, Kolmogorov–Smirnov test)			Probability mean(2020–2050)>			Probability mean(2070–2100)>			Means comparison (standardized differences)			Variance comparison (ratios)		
	ref/2020–2050	ref/2070–2100	2020–2050/2070–2100	mean(ref)	q75(ref)	q95(ref)	mean(ref)	q75(ref)	q95(ref)	2020/2050−ref	2070/2100−ref	2070/2100−2020/2050	2020/2050−ref	2070/2100−ref	2070/2100−2020/2050
French Alps, year	**0.00**	**0.00**	**0.00**	0.00	0.00	0.00	0.04	0.00	0.00	*−0.19*	*−0.26*	*−0.06*	**0.06**	*0.03*	*0.44*
French Alps, winter	**0.01**	**0.00**	**0.01**	0.72	0.61	0.44	0.87	0.80	0.70	*0.30*	*1.27*	*0.97*	**4.34**	*37.43*	*8.62*
French Alps, spring	**0.00**	**0.00**	**0.01**	0.01	0.00	0.00	0.00	0.00	0.00	*−0.43*	*−0.56*	**−0.13**	**0.41**	**0.20**	0.48
North. French Alps, year	**0.00**	**0.00**	0.07	0.00	0.00	0.00	0.00	0.00	0.00	*−0.44*	*−0.54*	**−0.10**	**0.31**	**0.24**	0.78
North. French Alps, winter	0.20	**0.00**	0.22	*0.32*	*0.10*	*0.00*	0.12	0.01	0.00	−0.10	*−0.21*	**−0.10**	0.62	**0.39**	0.63
North. French Alps, spring	**0.00**	**0.00**	**0.00**	0.01	0.00	0.00	0.00	0.00	0.00	*−0.42*	*−0.63*	*−0.22*	**0.45**	*0.22*	*0.49*
South. French Alps, year	**0.00**	**0.00**	0.36	0.02	0.00	0.00	0.00	0.00	0.00	*−0.30*	*−0.33*	*−0.03*	*0.11*	*0.03*	*0.29*
South. French Alps, winter	**0.05**	**0.00**	**0.03**	0.62	0.50	0.29	0.87	0.80	0.56	*0.31*	*0.95*	*0.64*	*7.05*	*24.32*	*3.45*
South. French Alps, spring	**0.00**	**0.00**	**0.00**	0.05	0.02	0.00	0.01	0.00	0.00	*−0.29*	*−0.36*	*−0.07*	*0.19*	*0.09*	*0.46*

Table 7. Changes in MEPRA index between the reference period and the two future periods. Ref, 2020–2050 and 2070–2100 correspond to the three considered periods: reference (1960–1990), mid and end of the 21st century, respectively. The probability for a future year to be higher than the reference mean and the 75 and 95 % percentiles of the reference distribution is quantified, as well as ratios and differences between the reference variance/mean and the two future variances/means, respectively. For the Kolmogorov Smirnov test, bold values indicate different samples at the 0.05 significance level. When the null hypothesis of similar underlying distributions is not rejected, exceedence probabilities appear in italic, as differences with the reference period may be insignificant. When the assumption of a Gaussian distribution is rejected for at least one of the considered samples, the significance of the variance comparison cannot be tested so that the variance ratios appear in italic. When the assumption of Gaussian distributions with similar variances is rejected for at least one of the considered samples, the significance of the mean comparison cannot be tested so that the mean standardized difference appears in italic. When the significance of variance/mean comparisons could be tested, ratios/standardized differences rejecting the null hypothesis of equality are shown in bold.

	Distribution comparison (p value, Kolmogorov–Smirnov test)			Probability mean(2020–2050)>			Probability mean(2070–2100)>			Means comparison (standardized differences)			Variance comparison (ratios)		
	ref/2020–2050	ref/2070–2100	2020–2050/ 2070–2100	mean(ref)	q75(ref)	q95(ref)	mean(ref)	q75(ref)	q95(ref)	2020/2050−ref	2070/2100−ref	2070/2100− 2020/2050	2020/2050−ref	2070/2100−ref	2070/2100− 2020/2050
French Alps, year	0.34	**0.00**	**0.00**	0.37	0.17	0.01	0.05	0.01	0.00	−0.08	**−0.31**	**−0.23**	0.93	0.53	0.58
French Alps, winter	0.20	**0.00**	0.17	0.33	0.16	0.00	0.13	0.03	0.00	−0.08	**−0.18**	−0.09	0.77	0.49	0.65
French Alps, spring	0.34	**0.01**	**0.00**	0.59	0.34	0.08	0.20	0.05	0.00	0.08	**−0.23**	**−0.31**	1.21	0.75	0.62
North. French Alps, year	0.54	**0.00**	**0.00**	0.44	0.26	0.02	0.09	0.02	0.00	−0.04	**−0.26**	**−0.22**	1.01	0.59	0.58
North. French Alps, winter	0.54	**0.02**	0.18	0.39	0.20	0.00	0.16	0.05	0.00	−0.06	**−0.16**	**−0.10**	0.83	0.52	0.62
North. French Alps, spring	0.20	0.13	**0.03**	0.65	0.39	0.14	*0.29*	*0.08*	*0.01*	0.12	**−0.14**	**−0.26**	1.39	0.91	0.66
South. French Alps, year	**0.00**	**0.00**	**0.00**	*0.32*	*0.20*	*0.08*	0.19	0.10	0.03	*−0.16*	*−0.31*	*−0.15*	*0.87*	*0.55*	*0.63*
South. French Alps, winter	**0.03**	**0.00**	0.37	*0.27*	*0.15*	*0.02*	0.21	0.10	0.01	*−0.17*	*−0.23*	*−0.06*	*0.65*	*0.49*	*0.76*
South. French Alps, spring	0.54	**0.00**	**0.00**	0.38	0.24	0.08	0.18	0.10	0.01	*−0.05*	*−0.25*	*−0.20*	*1.17*	*0.68*	*0.58*

Table 8. Changes in snow and climate multivariate distributions corresponding to each CI model, p values of the Cramer test. Bold values are lower than 0.05, indicating significant differences.

	Reference vs. 2020–2050	Reference vs. 2070–2100	2020–2050 vs. 2070–2100
French Alps, year	**$< 10^{-3}$**	**$< 10^{-3}$**	**$< 10^{-3}$**
French Alps, winter	**0.03**	**$< 10^{-3}$**	**0.02**
French Alps, spring	**$< 10^{-3}$**	**$< 10^{-3}$**	**0.002**
North. French Alps, year	**$< 10^{-3}$**	**$< 10^{-3}$**	**$< 10^{-3}$**
North. French Alps, winter	0.13	**$< 10^{-3}$**	0.08
North. French Alps, spring	**0.03**	**$< 10^{-3}$**	**0.003**
South. French Alps, year	**$< 10^{-3}$**	**$< 10^{-3}$**	**$< 10^{-3}$**
South. French Alps, winter	0.1	**0.02**	0.09
South. French Alps, spring	**$< 10^{-3}$**	**$< 10^{-3}$**	**$< 10^{-3}$**

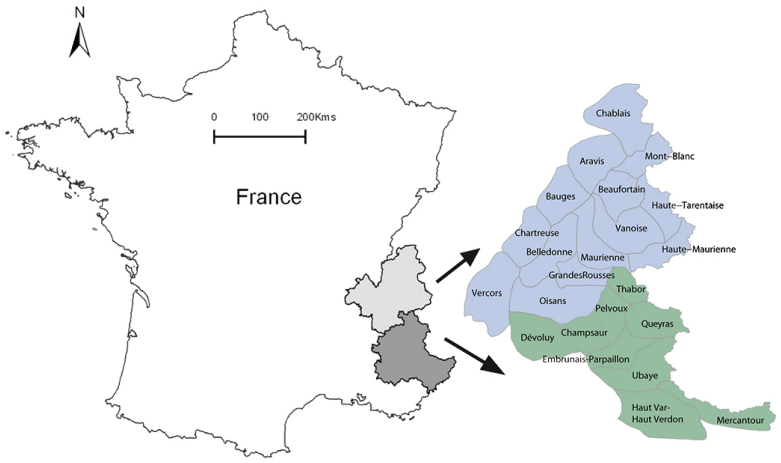

Fig. 1. Area studied. The French Alps are divided into 23 massifs. The Northern French Alps and Southern French Alps are represented in blue and green, respectively.

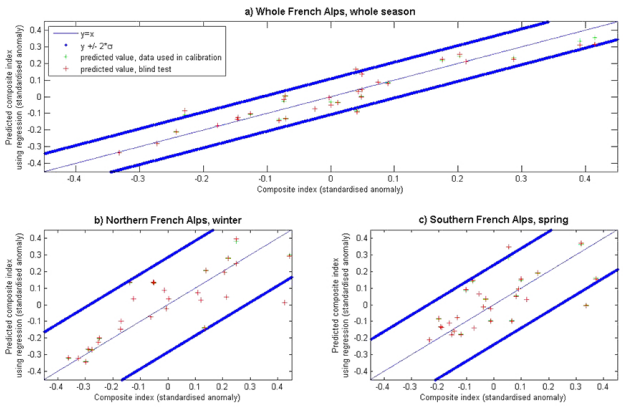

Fig. 2. Cross validation of the composite index regression model: entire French Alps for the full avalanche year **(a)**, Northern French Alps in winter sub-season **(b)** and Southern French Alps in spring sub-season **(c)**. In each panel, the predictive performance is assessed with/without (leave-one-out scheme) each pseudo-observation. To represent predictive uncertainty around the first bisector, the classical ± two standard deviations wide bandwidth is drawn.

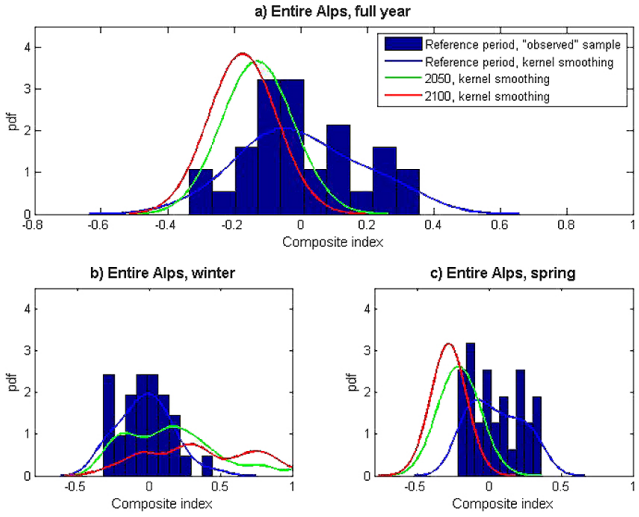

Fig. 3. Distribution of the annual and seasonal means of the CI regression model over the reference period and in 2020–50 and 2070–2100. The entire French Alps are considered, during the full avalanche year **(a)** and during winter **(b)** and spring **(c)** sub-periods.

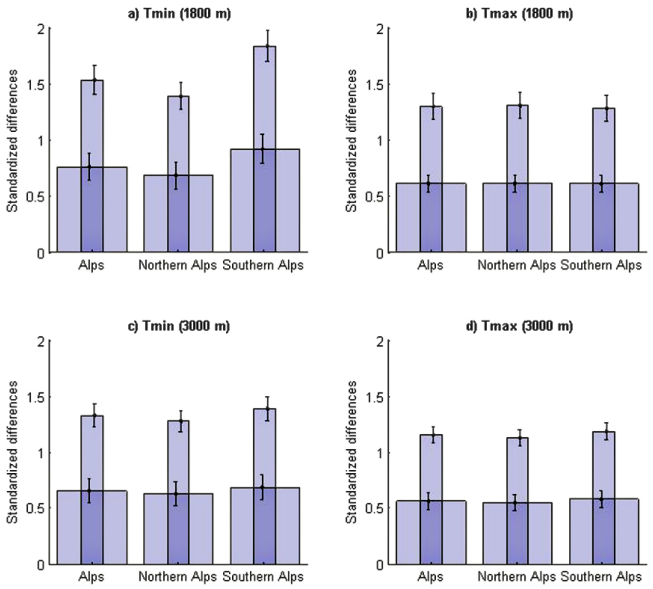

Fig. 4. Standardized differences (differences between reference and future period means divided by the variability range for the reference period) in temperatures (minimal/maximal, at 1800 and 3000 m a.s.l.) at the entire French Alps scale for the mid and end of the 21st century (respectively ~~large~~ and thin bars) for the A1B scenario. Error bars (±1.5 σ) represent interannual variability.

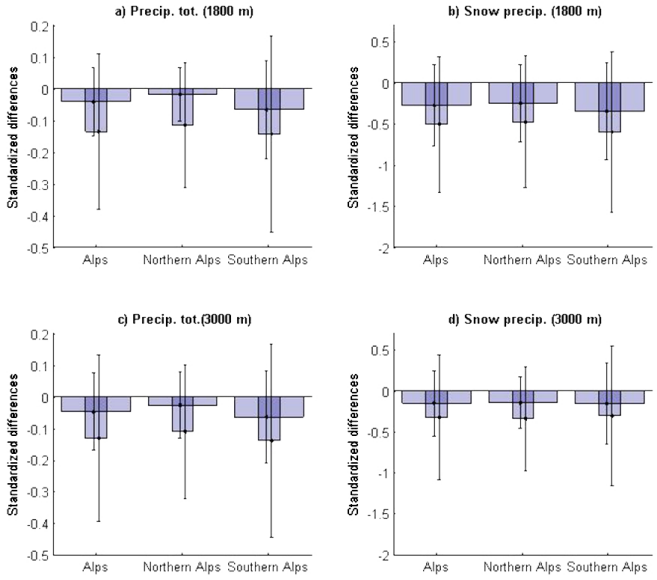

Fig. 5. Standardized differences (differences between reference and future period means divided by the variability range for the reference period) in precipitation (total/snow, at 1800 and 3000 m a.s.l.) at the entire French Alps scale for the mid and end of the 21st century (respectively large and thin bars) for the A1B scenario. Error bars (±1.5 σ) represent interannual variability.

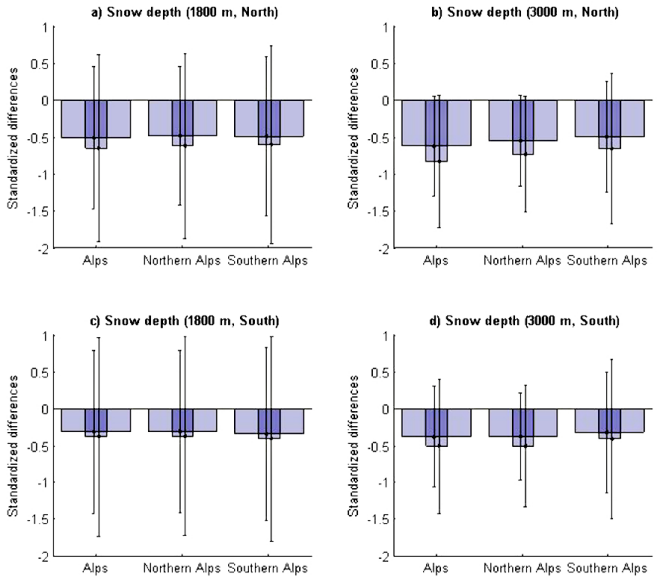

Fig. 6. Standardized differences (differences between reference and future period means divided by the variability range for the reference period) in total snow depth (north and south facing slope, at 1800 and 3000 m a.s.l.) at the entire French Alps scale for the mid and end of the 21st century (respectively large and thin bars) for the A1B scenario. Error bars (±1.5 σ) represent interannual variability.

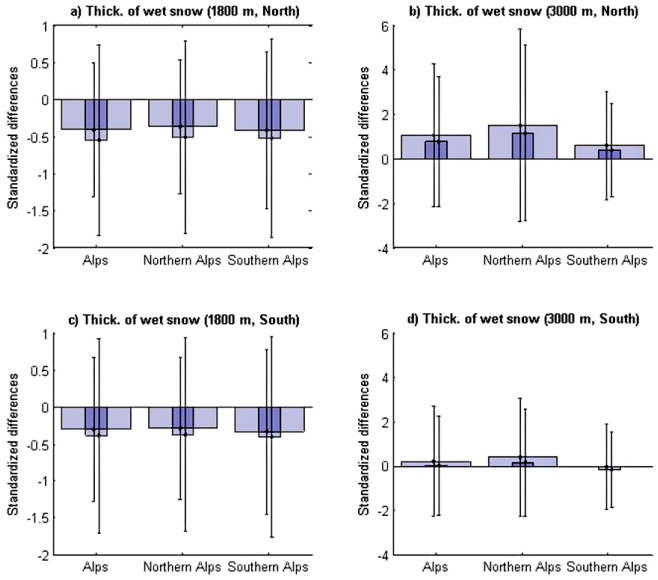

Fig. 7. Standardized differences (differences between reference and future period means divided by the variability range for the reference period) in thickness of wet snow (north and south facing slope, at 1800 and 3000 m a.s.l.) at the entire French Alps scale for the mid and end of the 21st century (respectively large and thin bars) for the A1B scenario. Error bars (±1.5 σ) represent interannual variability.

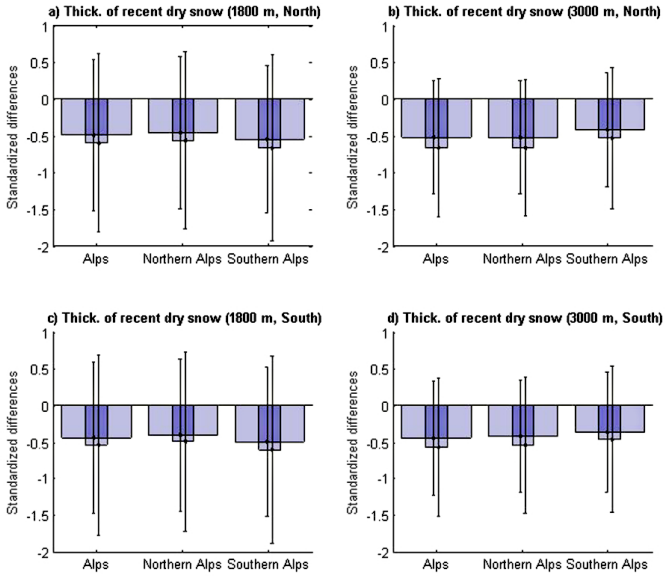

Fig. 8. Standardized differences (differences between reference and future period means divided by the variability range for the reference period) in thickness of recent surface dry snow (north and south facing slope, at 1800 and 3000 m a.s.l.) at the entire French Alps scale for the mid and end of the 21st century (respectively large and thin bars) for the A1B scenario. Error bars (±1.5 σ) represent interannual variability.

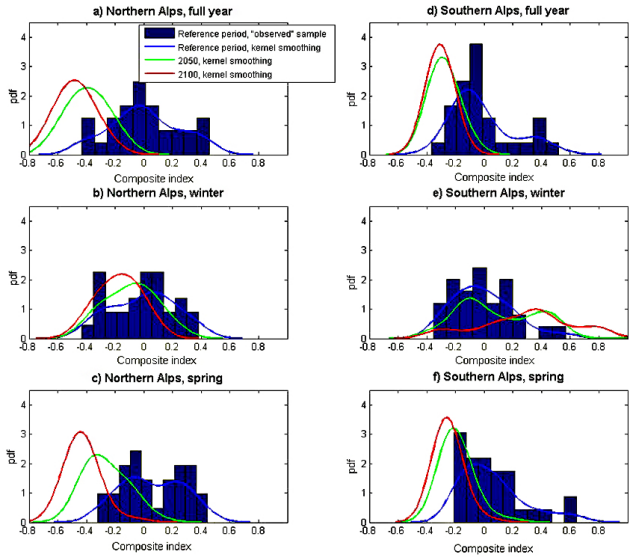

Fig. 9. Distribution of the Composite Index during reference and future periods 2020-and 2070–2100. Northern (left panel) and Southern (right panel) French Alps during the full avalanche year **(a–d)** winter **(b–e)** and spring **(c–f)** sub-periods.

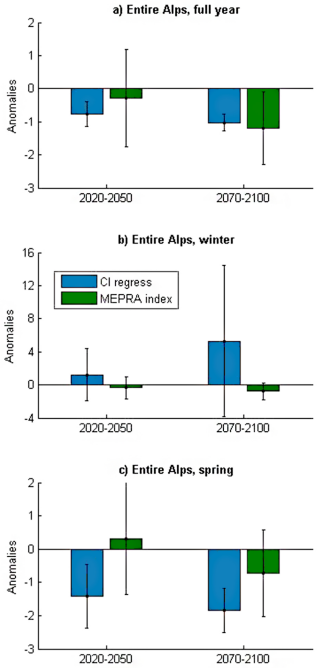

Fig. 10. Changes in MEPRA index vs. changes in Composite Index regression model (anomalies with the reference period) at the entire French Alps scale for the full avalanche year **(a)**, and winter **(b)** and spring **(c)** sub-periods.

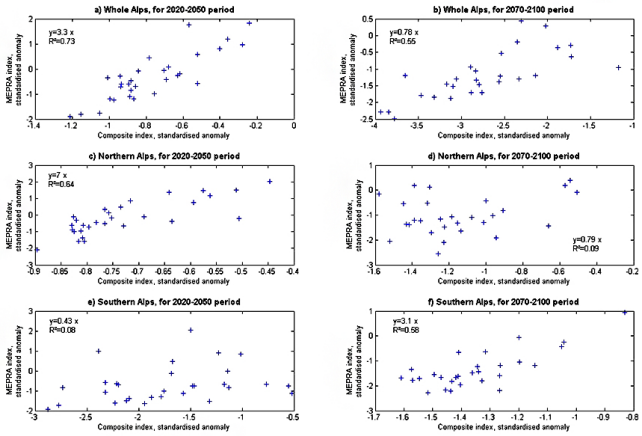

Fig. 11. Scatter plots of standardized changes (with regard to reference period) in the MEPRA index vs. the CI regression model. Future periods 2020–2050 and 2070–2100 are respectively considered in left and right panels. Subplots **(a)** and **(b)** concern the whole French Alps, **(c)** and **(d)** the Northern French Alps and **(e)** and **(f)** the Southern French Alps.

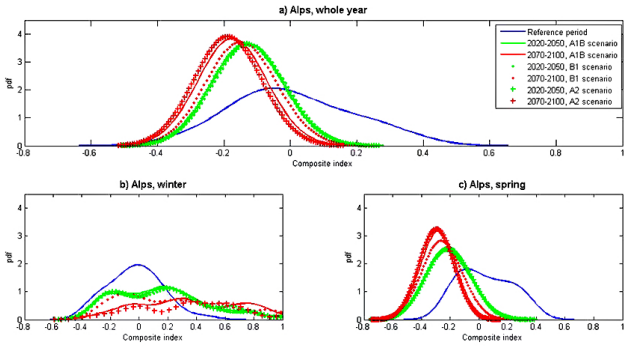

Fig. 12. Distribution of the CI regression model for three IPCC scenarios for the mid and end of the 21st at the entire French Alps **(a)**, Northern **(b)** and Southern **(c)** French Alps scales.